The National Ignition Facility (NIF) and High Energy Density Science Research at LLNL

Presentation to:
IEEE Pulsed Power and Plasma Science Conference

C. J. Keane
Director, NIF User Office
June 21, 2013

Lawrence Livermore National Laboratory
This work performed under the auspices of the U.S. Department of Energy by Lawrence Livermore National Laboratory under Contract DE-AC52-07NA27344

978-1-4673-5168-3/13/$31.00 ©2013 IEEE

Report Documentation Page

Form Approved
OMB No. 0704-0188

1. REPORT DATE **JUN 2013**	2. REPORT TYPE **N/A**	3. DATES COVERED **-**

4. TITLE AND SUBTITLE **The National Ignition Facility (NIF) and High Energy Density Science Research at LLNL**	5a. CONTRACT NUMBER 5b. GRANT NUMBER 5c. PROGRAM ELEMENT NUMBER
6. AUTHOR(S)	5d. PROJECT NUMBER 5e. TASK NUMBER 5f. WORK UNIT NUMBER
7. PERFORMING ORGANIZATION NAME(S) AND ADDRESS(ES) **Lawrence Livermore National Laboratory**	8. PERFORMING ORGANIZATION REPORT NUMBER
9. SPONSORING/MONITORING AGENCY NAME(S) AND ADDRESS(ES)	10. SPONSOR/MONITOR'S ACRONYM(S) 11. SPONSOR/MONITOR'S REPORT NUMBER(S)

12. DISTRIBUTION/AVAILABILITY STATEMENT
Approved for public release, distribution unlimited

13. SUPPLEMENTARY NOTES
See also ADM002371. 2013 IEEE Pulsed Power Conference, Digest of Technical Papers 1976-2013, and Abstracts of the 2013 IEEE International Conference on Plasma Science. IEEE International Pulsed Power Conference (19th). Held in San Francisco, CA on 16-21 June 2013., The original document contains color images.

14. ABSTRACT

15. SUBJECT TERMS

16. SECURITY CLASSIFICATION OF:			17. LIMITATION OF ABSTRACT	18. NUMBER OF PAGES	19a. NAME OF RESPONSIBLE PERSON
a. REPORT **unclassified**	b. ABSTRACT **unclassified**	c. THIS PAGE **unclassified**	**SAR**	**78**	

Standard Form 298 (Rev. 8-98)
Prescribed by ANSI Std Z39-18

Advances in laser/pulsed power drivers and related simulation, diagnostic, and other capabilities enable exciting new opportunities for scientific discovery

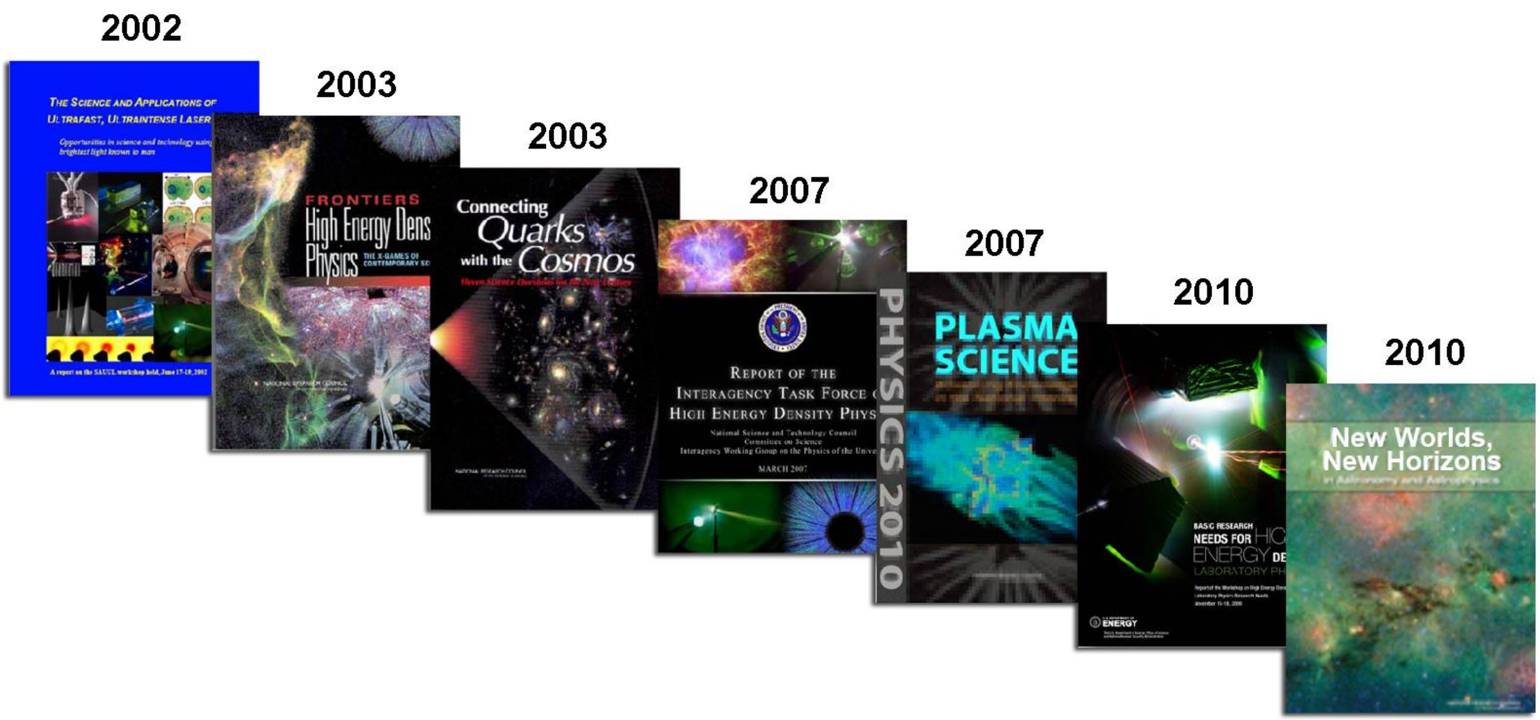

- **"Science on (NIF, Omega, Jupiter, Z,…) science is more than HED science"**

2003 NRC Report on High Energy Density Physics defines HED science as P> 1 Mbar (10^{11} J/m^3)

Hydrogen Molecule

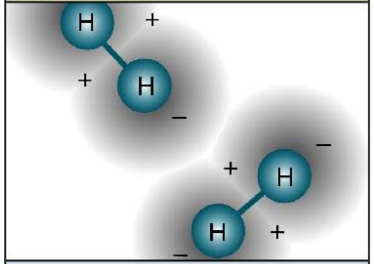

Binding energy ~10^{11} J/m^3

Jupiter

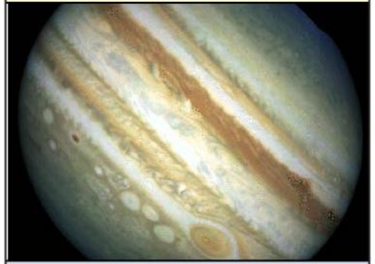

P ~ 80 MBar (core)

Sun

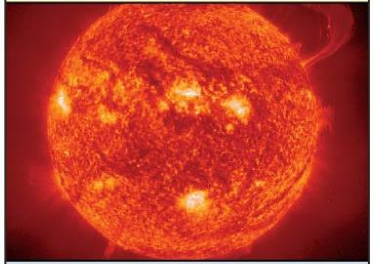

P ~ 3x105 MBar (core)

Fusion Target

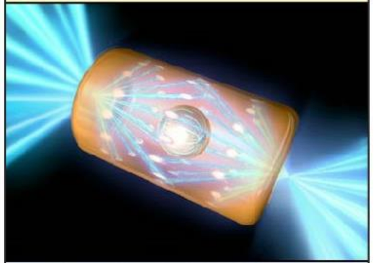

P ~ 2x106 MBar (peak burn)

1 atm = .98 Bar

00ABC/lch • NIF-0110-18321s1s2

Advances in drivers, diagnostics, targets, and simulation are driving evolution of this field worldwide

HiPER (EU)

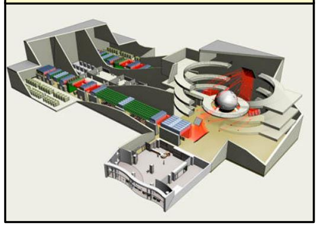

LMJ (France)

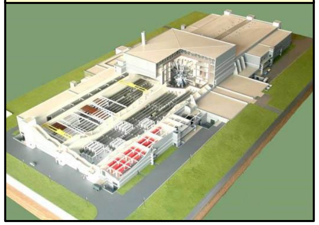

NIF Laser

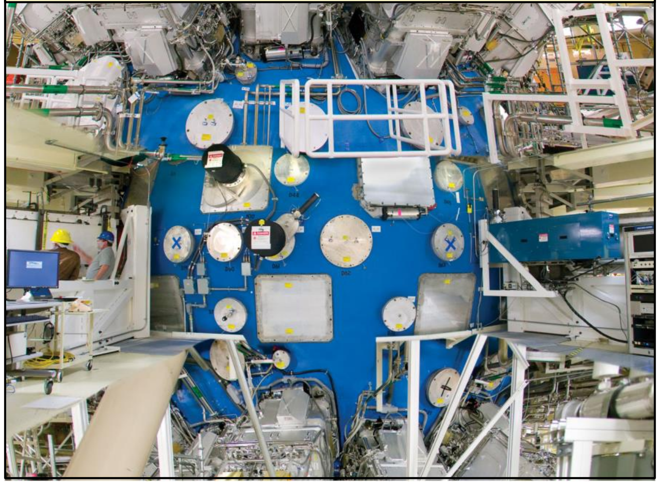

ORION (UK)

Vulcan (UK)

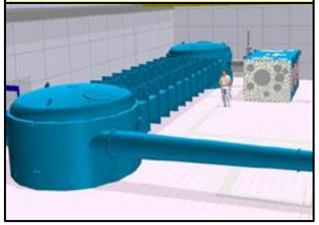

SG-III (China)

FIREX (Japan)

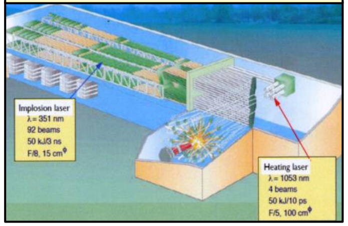

UFL-2M (Russia)

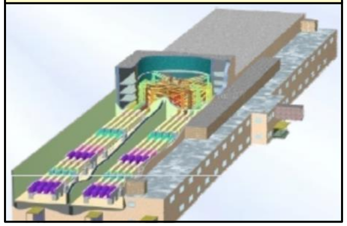

The NIF and Jupiter lasers are the primary HED facilities at LLNL

Jupiter

“Intermediate scale” facility ideal for student training

NIF

Large-scale facility for high energy applications

Jupiter Laser Facility

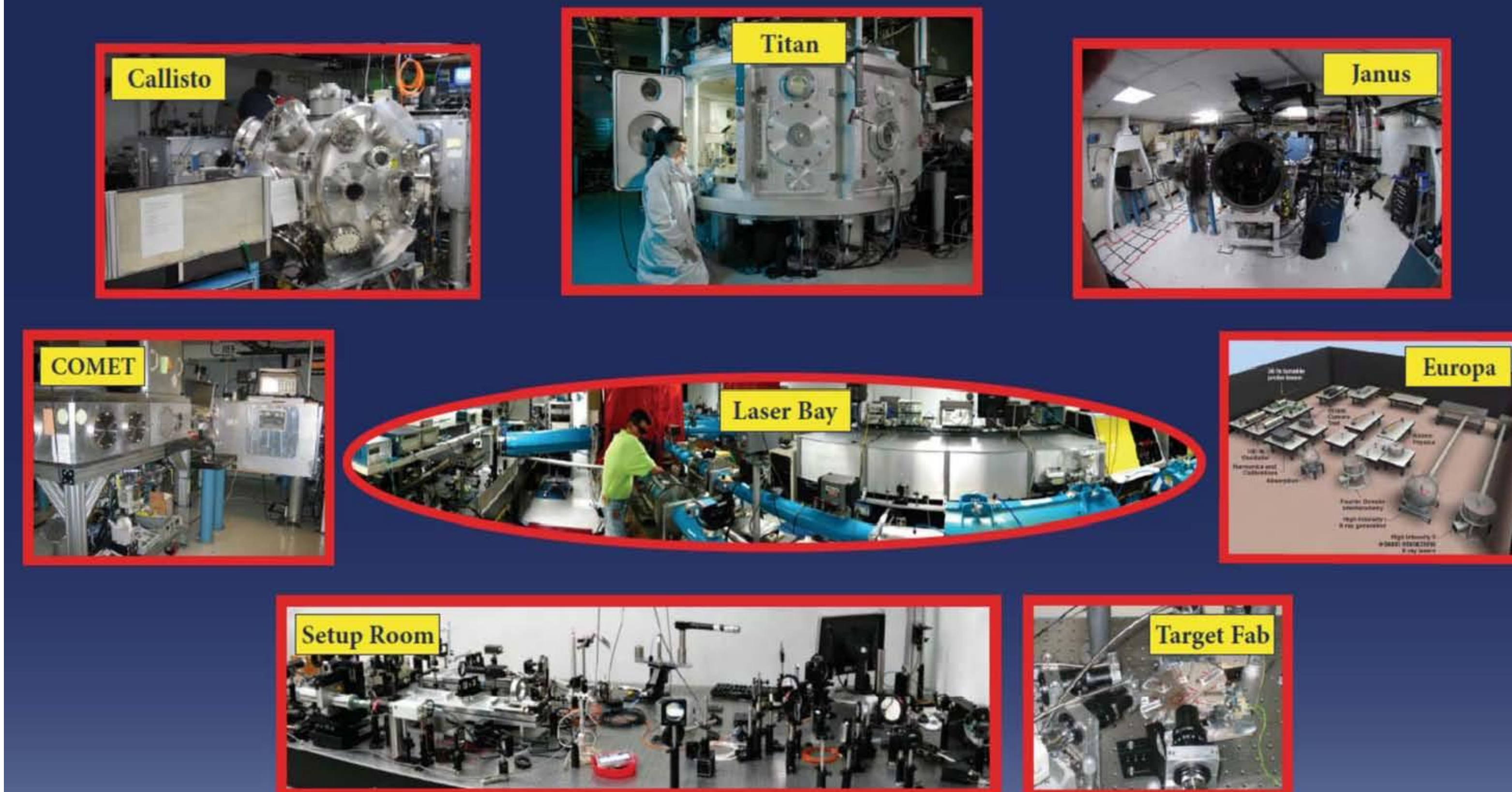

Expanding High Energy-Density Science

6

Jupiter has operated as a user facility since 2008, with 112 peer-reviewed publications through FY2012

COMET is used by NIF to calibrate and test diagnostics

Studies of the mechanisms of powerful terahertz radiation from laser plasmas

Yutong Li* , Guoqian Liao*, Weimin Wang*, Chun Li*, Luning Su*, Yi Zheng*, Meng Liu*, Wenchao Yan*, Mulin Zhou*, Fei Du*, J. Dunn**, J. Hunter**, J. Nilsen**, Zhengming Sheng***, Jie Zhang***

* Beijing National Laboratory for Condensed Matter Physics, Institute of Physics, Chinese Academy of Sciences, Beijing 100190, China

** Lawrence Livermore National Laboratory, 7000 East Avenue, Livermore, CA 94551, USA

*** Key Laboratory for Laser Plasmas (MoE) and Department of Physics, Shanghai Jiao Tong University, Shanghai 200240, China

Recently Terahertz (THz) radiation from laser-produced plasmas has attracted much interest since plasmas can work at arbitrarily high laser intensity. This paper will discuss the generation mechanisms of plasma-based THz radiation.

I. INTRODUCTION

Terahertz radiation has been attracted much interest due to increasingly wide applications. Though THz radiation can be generated with various ways, it is still a big challenge to obtain strong tabletop sources. Plasmas, with an advantage of no damage limit, are promising medium to generate strong THz radiation [1]. THz radiation from femtosecond laser-induced plasma filaments in low density gases (particularly in air) has been reported. However, the radiation is found to be saturated with pump laser intensity. Recently THz radiation from intense laser-solid interactions has also been demonstrated. In principle, for solid targets the laser intensity can be arbitrarily high. The typical intensity of a multi-terawatt laser system is higher than 10^{18} W/cm^2 (up to 10^{21} W/cm^2 with a Petawatt laser). Using such ultraintense lasers, strong THz radiation with energies even up to mJ is expected. Intense laser-plasma interactions provide new opportunity to greatly enhance the THz source strength. On the other hand, the THz radiation can also be used as a new way to diagnose the interactions.

We have symmetrically studied strong THz radiation from solid targets driven by relativistic laser pulses. The experiments were carried out using femtosecond and picosecond laser systems, respectively. THz radiation with a pulse energy of tens μJ/sr (driven by femtosecond laser), even ~mJ/sr (driven by picosecond laser) is observed. In this talk, the THz polarization, temporal waveform, angular distribution and energy dependence on the laser energy will be presented. We find that the radiation is dependent on the preplasma density scale length. We believe that The THz radiation is probably attributed to the self-organized transient fast electron currents formed along the target surface for steep plasma density profile, while, the linear mode conversion mechanism when a large scale preplasma is presented.

II. THZ RADIATION FROM FEMTOSECOND LASER –SOLID INTERACTIONS FOR STEEP PLASMM PROFILE

Hamster *et al.* first demonstrated the generation of THz pulses with energies of 1 μJ/sr from solid aluminum targets irradiated by laser pulses at an intensity ~10^{19} W/cm^2 [2]. They believed that the THz radiation originated from the charge separation fields arisen from the longitudinal ponderomotive force at the critical density surface. THz pulses with 0.5 μJ/sr were also observed by Sagisaka *et al.* from Ti solid foil targets at a little bit lower laser intensity 10^{17} W/cm^2 [3]. They proposed an "antenna" model to explain the observation, in which assumes that the electrons spread over the whole target and the target acts like an antenna. The spectrum of THz radiation from laser driven plasmas generated on a copper wire was measured using free-space electro-optic sampling by Gao *et al.* [4]. However, no clear evidence was found to show that the target size affects the THz radiation spectrum.

Our femtosecond experiments were carried out using the Xtreme Light II (XL-II) Ti: sapphire laser system at the Institute of Physics of the Chinese Academy of Sciences. A linearly-polarized laser pulse with an energy up to 150 mJ in 100 fs at 800 nm was focused onto a 30 *μ*m thick copper foil at an incidence angle 67.5° using an *f*/3.5 off-axis parabolic mirror. A calibrated thermoelectric detector aligned in the laser specular direction was used to measure the THz pulse energy. Figure 1(a) shows the dependence of the THz pulse energy on pump laser energy. Each data point is taken by an average of ~10 shots. The energy of the THz radiation monotonically increases with laser energy. For the laser energy of 130 mJ, the THz energy is up to 5.5 *μJ* in 0.11 sr. The temporal waveform was measured by a modified, single-shot electro-optic method with a chirped laser pulse, where a 1-mm thick ZnTe was used as the sampling crystal. It is found that the THz peak frequency is at about 0.5 THz. The frequency can be tuned by changing the laser incidence angle and plasma conditions.

The strong THz radiation observed indicated that a net current should have been excited in the plasma. In the interaction of a relativistic laser pulse with a solid foil, due to the confinement of the spontaneous quasistatic magnetic and electrostatic fields at target surface, a lateral

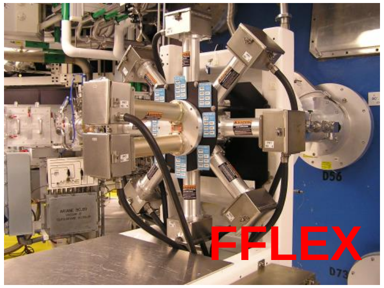

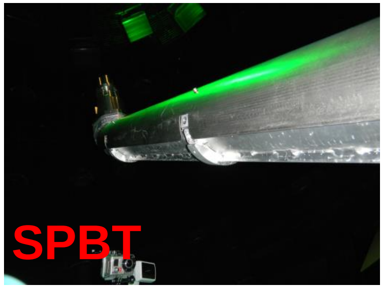

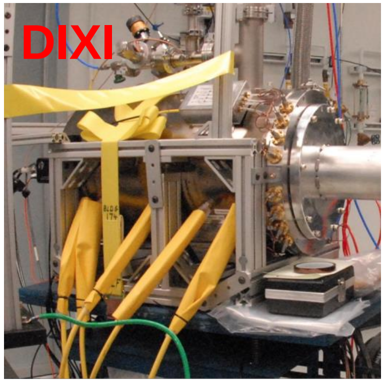

NIF/Jupiter User Group meeting: Feb. 10-13, 2013; approx. 200 attendees, 16 countries

Overview of NIF and JLF user communities

Jupiter registered users (FY2013)

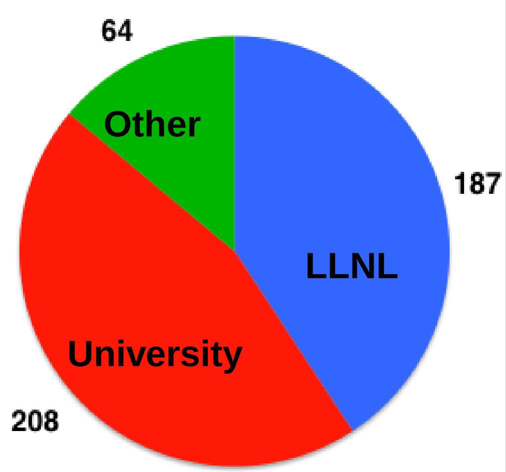

459 registered users, including 117 students

NIF User Group membership

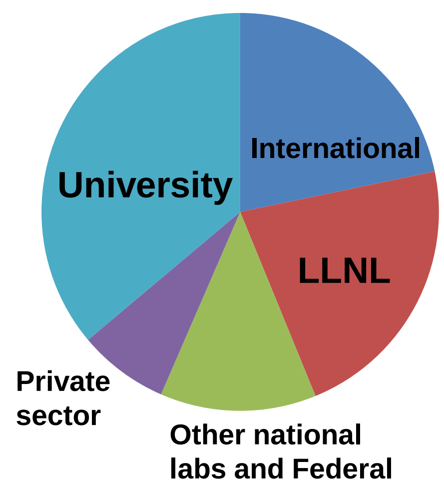

299 members total

NIF missions

Ensuring National Security

Advancing Frontier Science

Enabling Clean Energy

Building Future Generations of HED Scientists

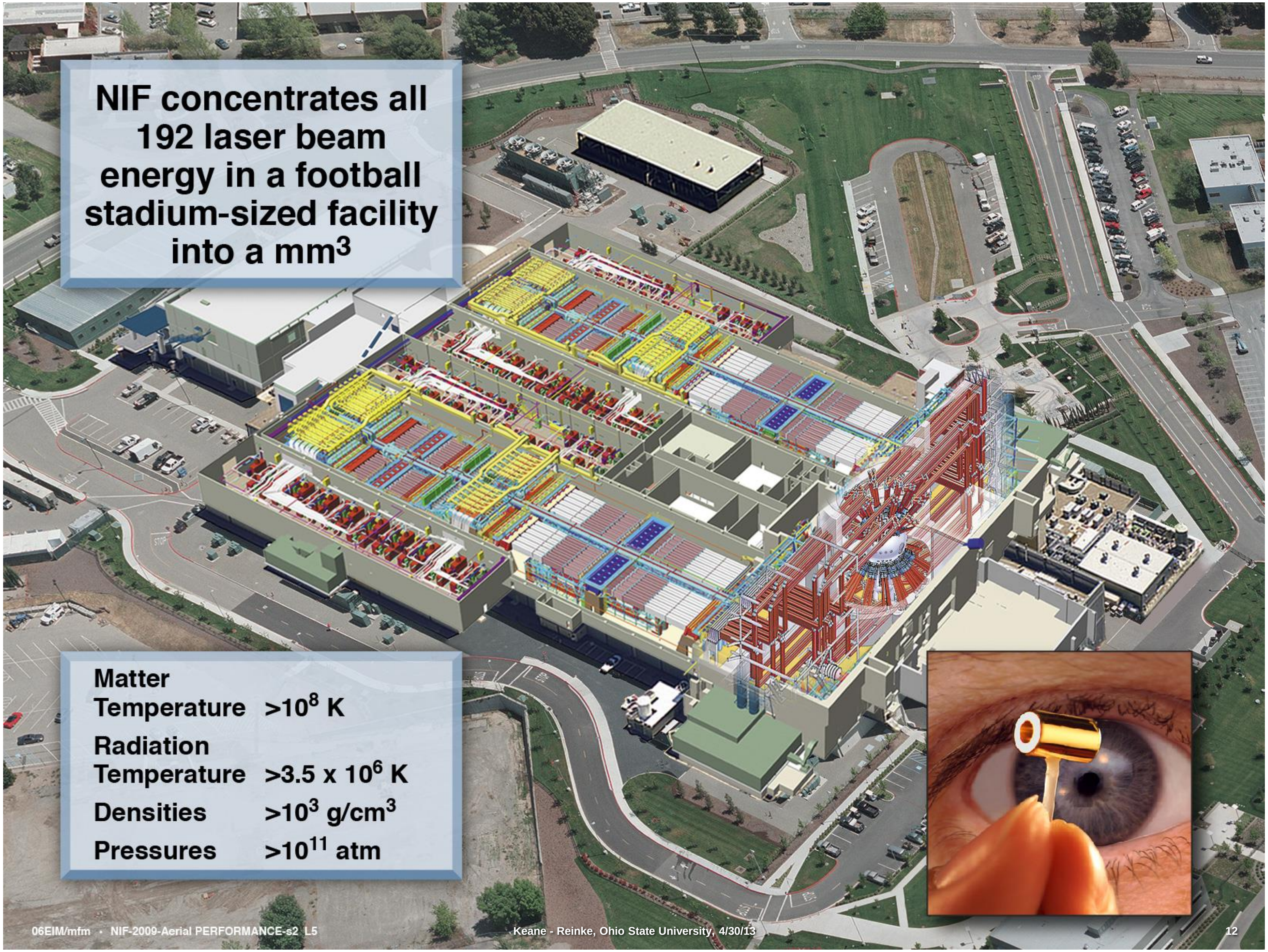
NIF concentrates all 192 laser beam energy in a football stadium-sized facility into a mm^3
Matter Temperature >10^8 K
Radiation Temperature >3.5×10^6 K
Densities >10^3 g/cm^3
Pressures >10^{11} atm
06EIM/mfm • NIF-2009-Aerial PERFORMANCE-s2 L5
Keane - Reinke, Ohio State University, 4/30/13
12

From relativistic phenomena to ~ 1 eV condensed matter physics- NIF allows a wide range of experiments

Laser

Wide variety of pulse shapes, w/ few percent reproducibility and precision (1.855 MJ/533 TW exceeds specs)

Diagnostics

Photon and particle diagnostics w/ high spatial, temporal, spectral resolution

Targets

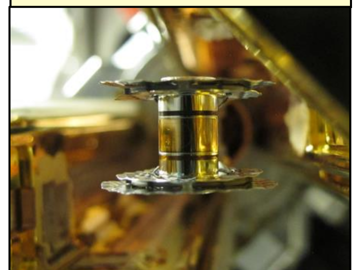

Spherical, planar, machined perturbations, exotic materials,..

Simulation

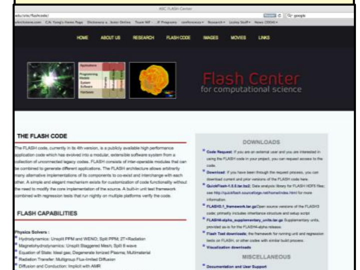

Experimental design via target and laser simulation tools

NIF will also bring an unprecedented new capability- the ability to study burning plasma physics


00ABC/lh • NIF-0609-16540s2
15


25 21
KONECRANES
00ABC/abc • NIF-0609-16740s2L2
2013-049951s2.ppt
16

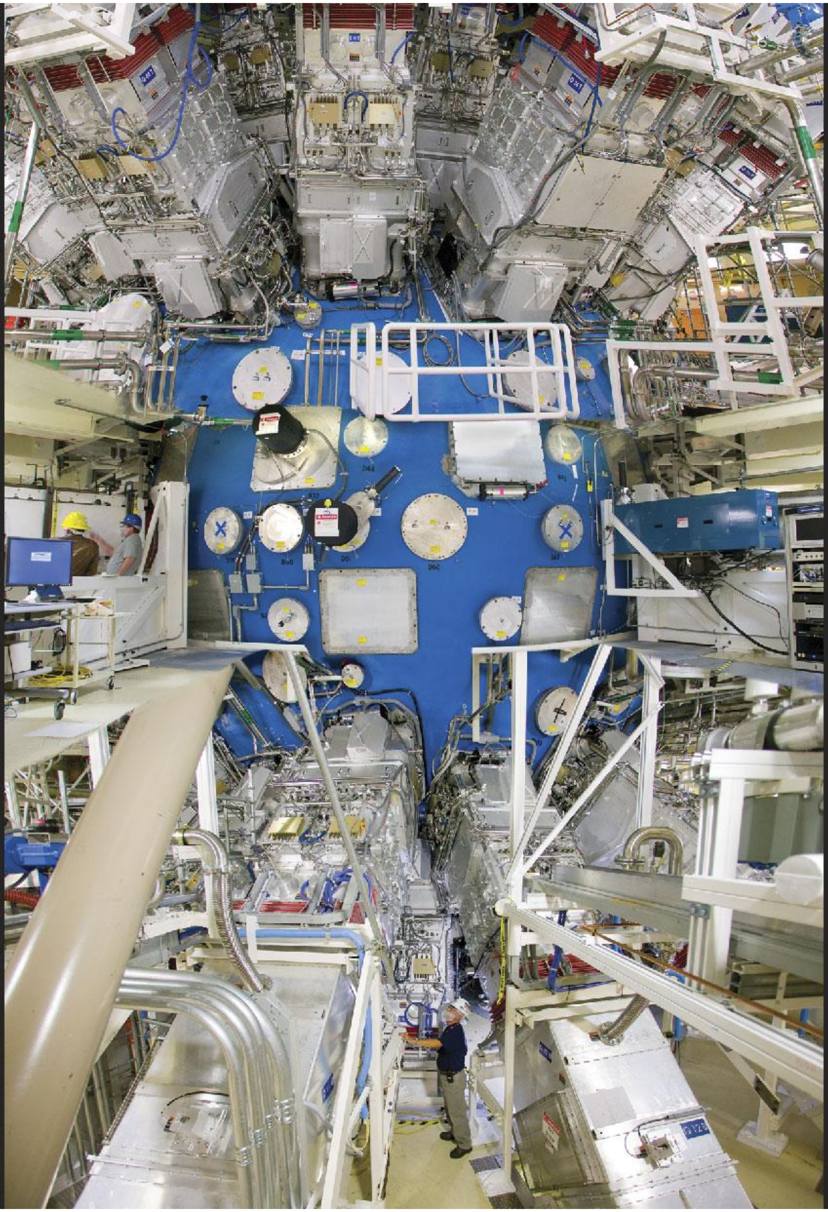

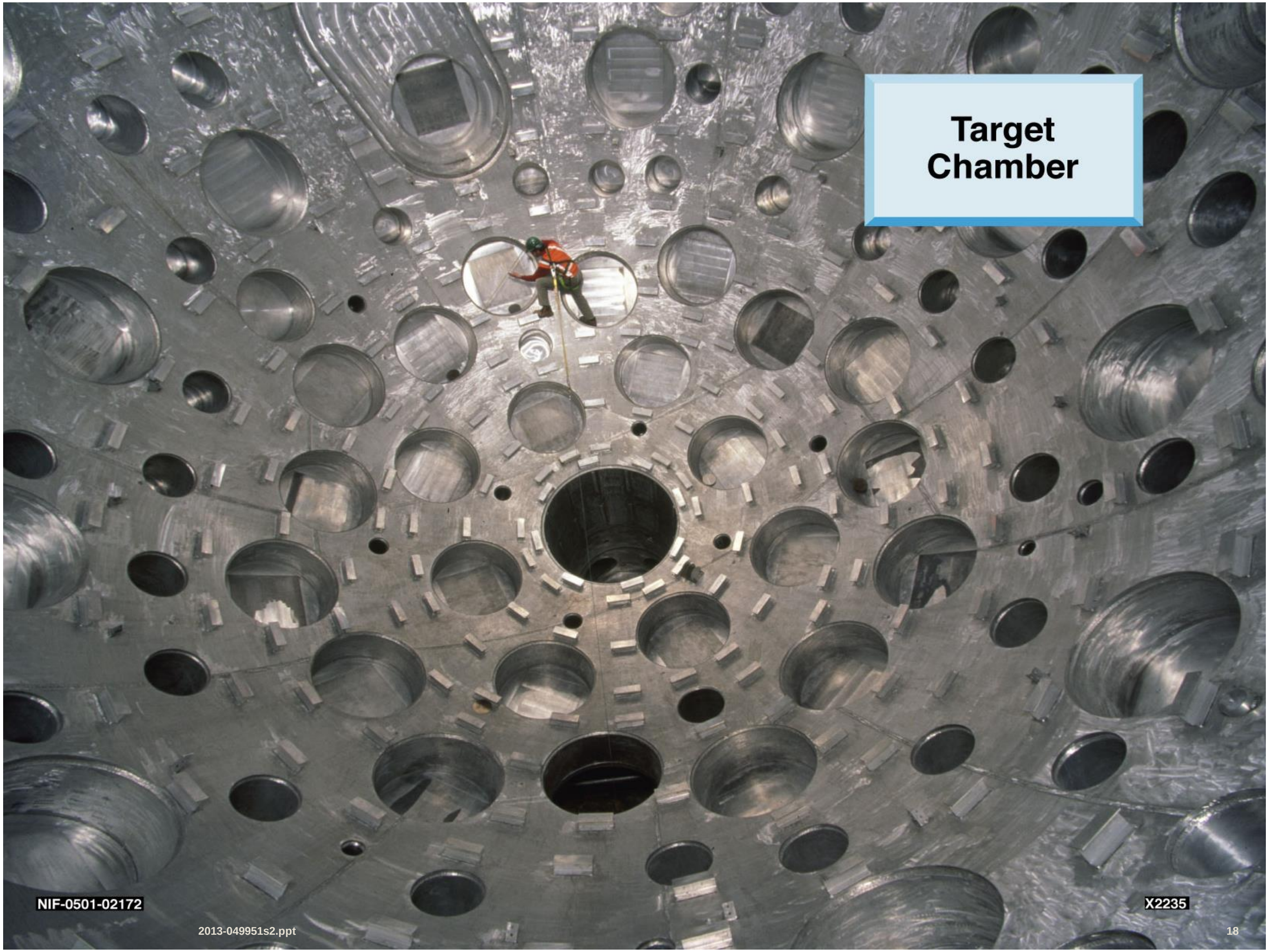
Target
Chamber
NIF-0501-02172
X2235
2013-049951s2.ppt
18

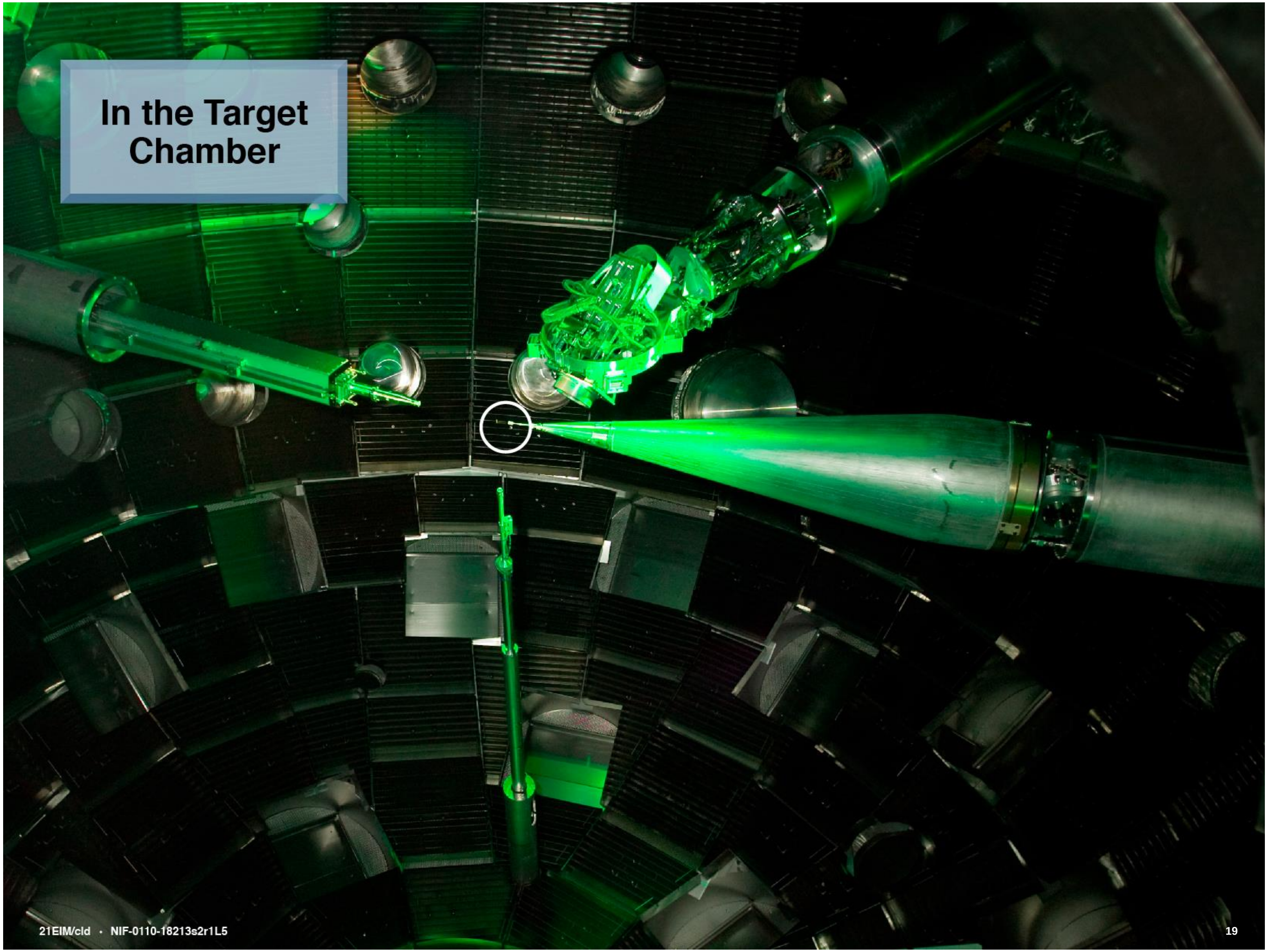
In the Target Chamber
21EIM/cld · NIF-0110-18213s2r1L5
19

NIF has met—and exceeded—its 1.8 MJ, 500 TW design specification

- **NIF Laser is operating 24/7 with exceptional reproducibility and reliability (99%)**
- **The NIF has intrinsic capability to continue on this growth path for several more years**

The laser energy and power available for experiments have been steadily increasing

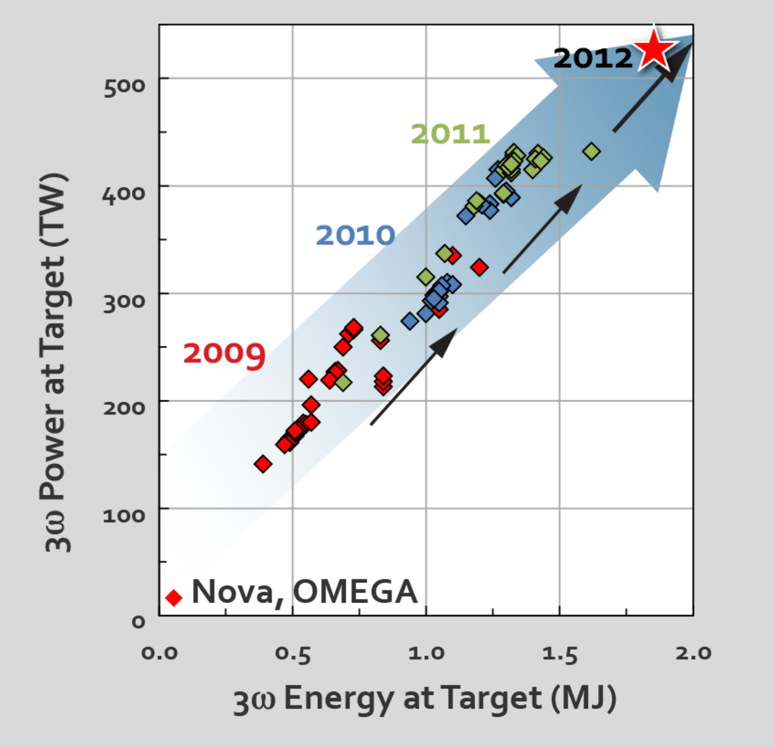

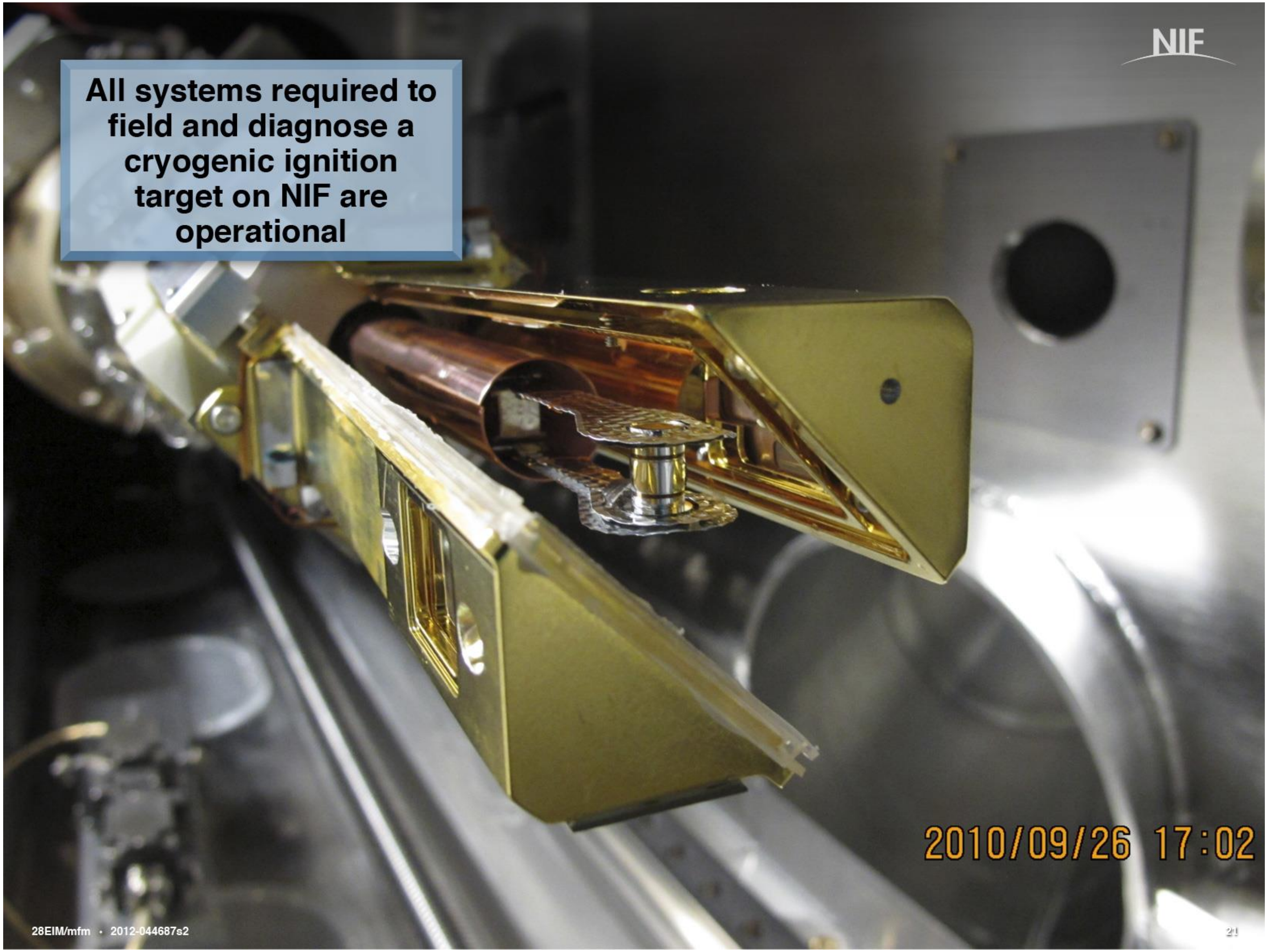
NIF
All systems required to field and diagnose a cryogenic ignition target on NIF are operational
2010/09/26 17:02
28EIM/mfm • 2012-044687s2
21

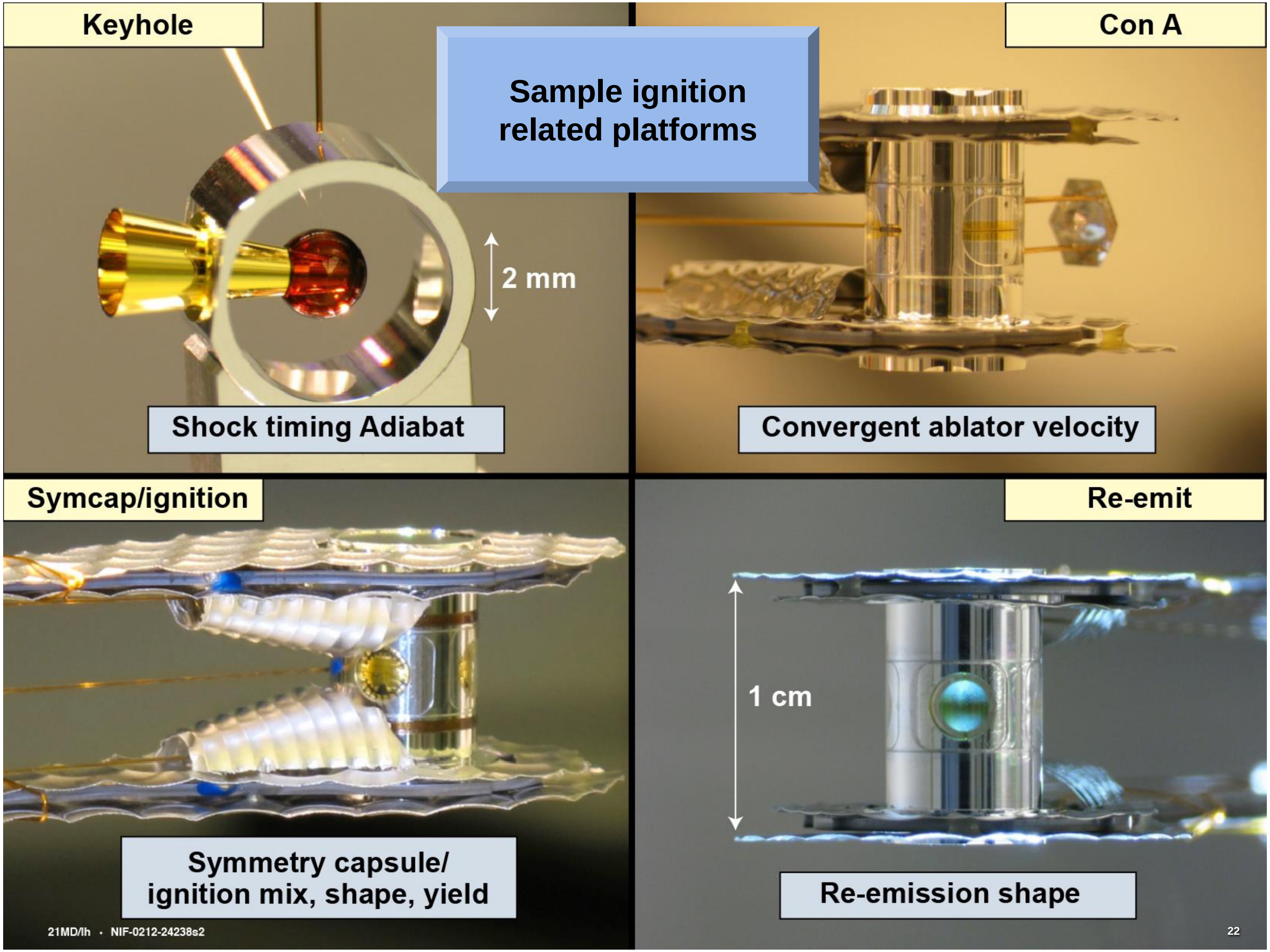
Keyhole
Sample ignition related platforms
Con A
2 mm
Shock timing Adiabat
Convergent ablator velocity
Symcap/ignition
Re-emit
1 cm
Symmetry capsule/ ignition mix, shape, yield
Re-emission shape
21MD/lh • NIF-0212-24238s2
22

63 target diagnostics enable cutting edge science on the NIF

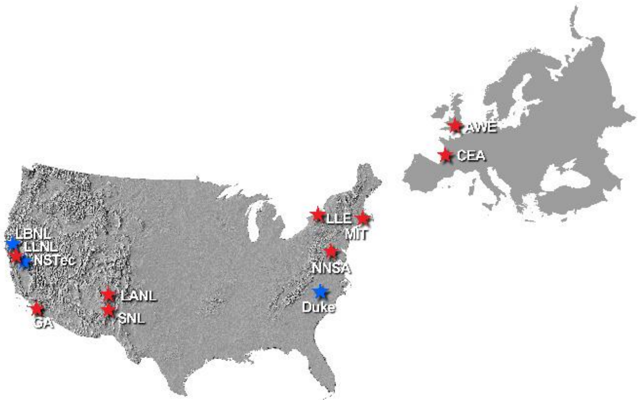

- LLNL
- LANL
- LLE
- NSTec
- U of M
- LBNL
- AWE
- MIT
- CEA
- Duke
- SNL
- GSI

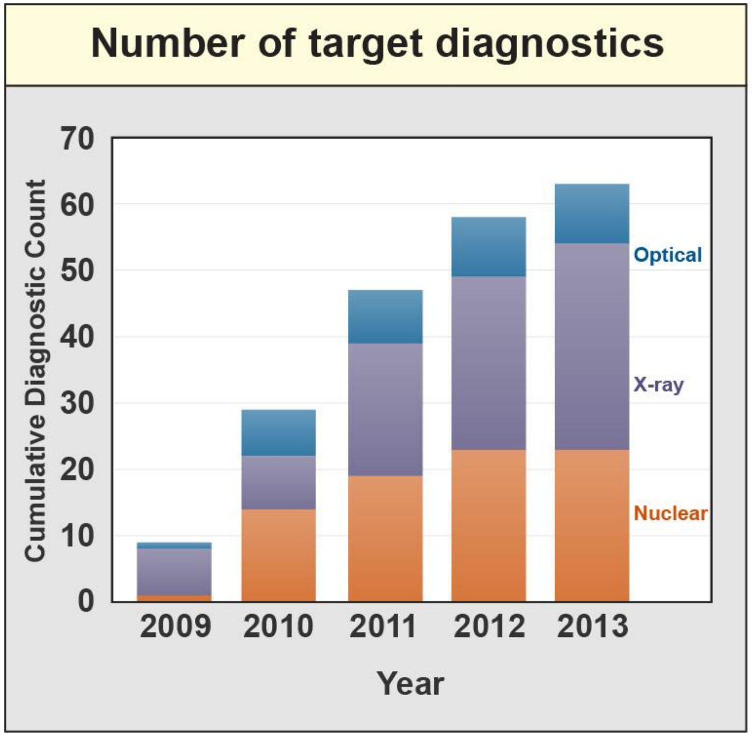

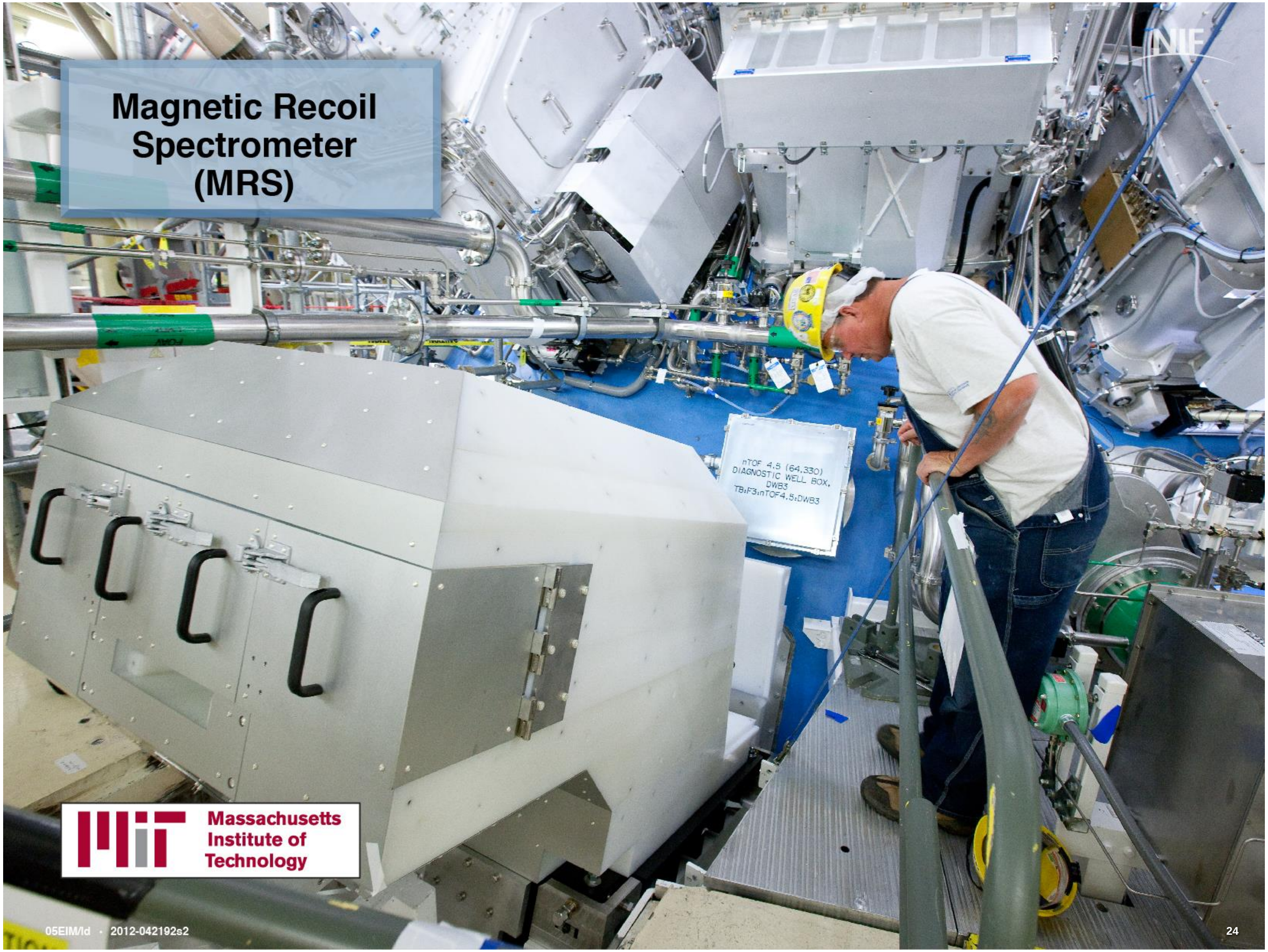
Magnetic Recoil Spectrometer (MRS)
NIF
nTOF 4.5 (64.330)
DIAGNOSTIC WELL BOX,
DWB3
TB:F3:nTOF4.5:DWB3
Massachusetts Institute of Technology
05EIM/ld · 2012-042192s2
24

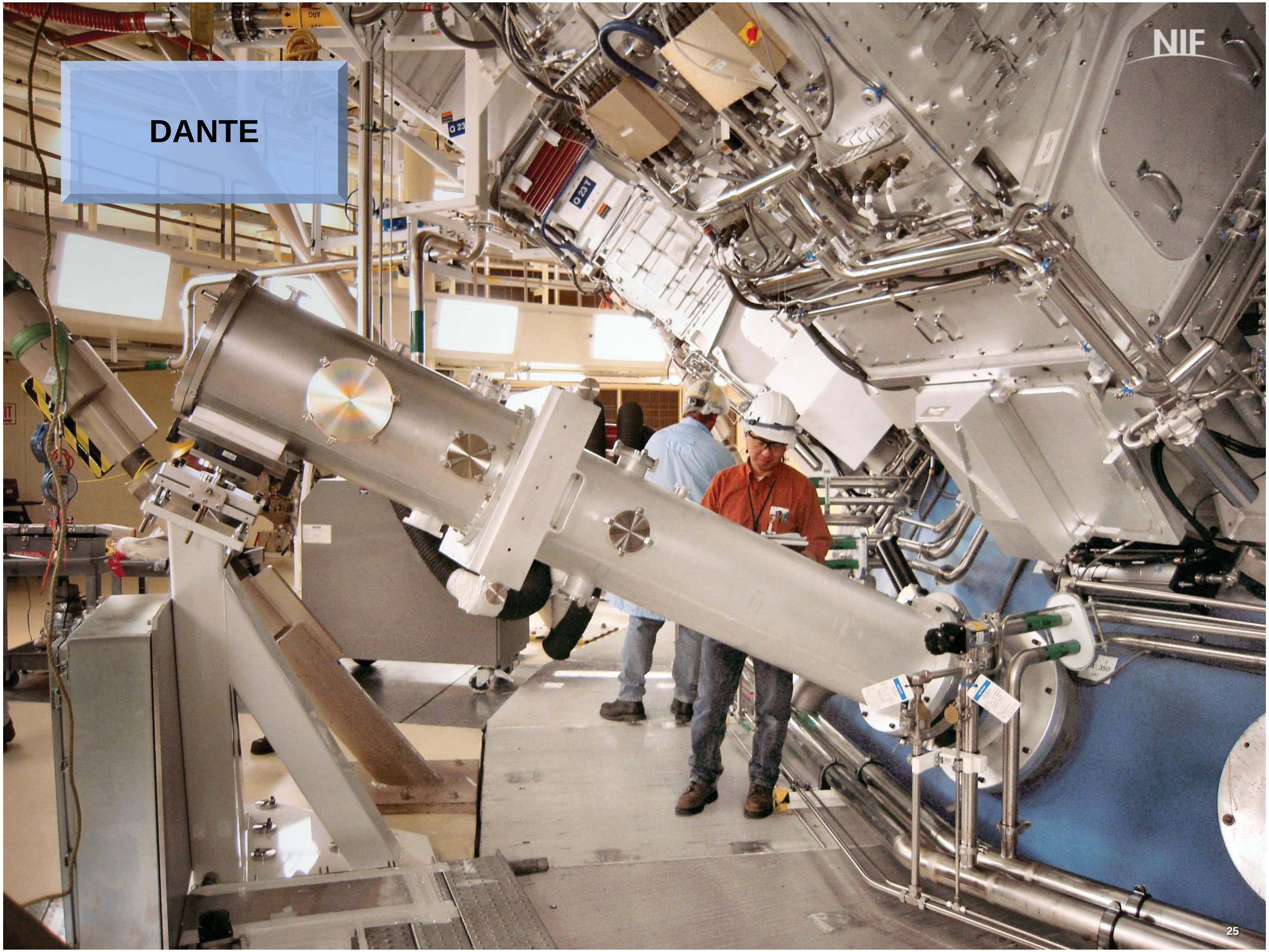
DANTE
NIF
25

Gamma Reaction History (GRH)

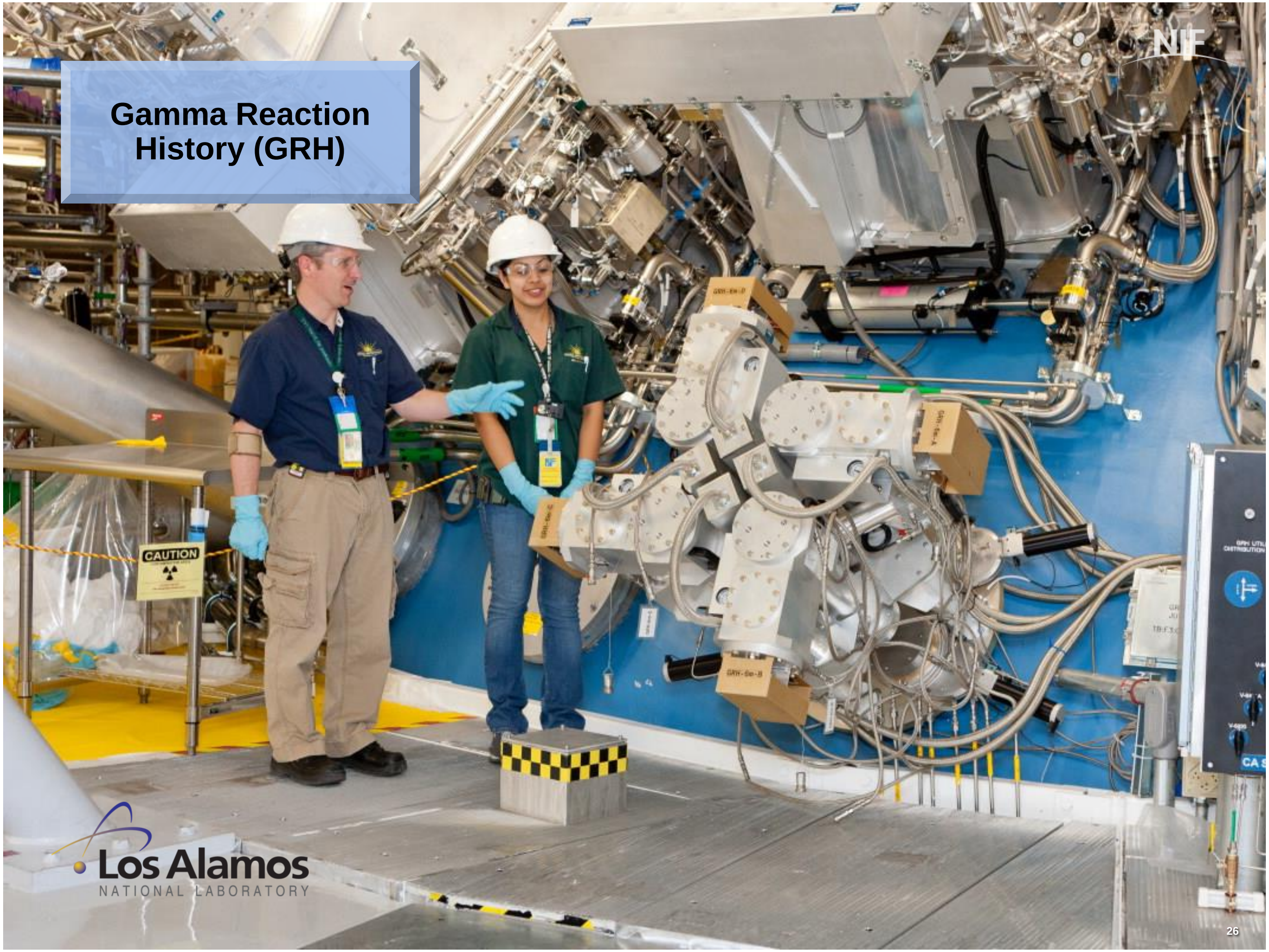

Advanced Radiographic Capability (ARC)
22EIM/sb · NIF-0910-20123s2
27


FFLEX
PMT NO. 9
PMT NO. 10
PMT NO. 4
WARNING
N28
D5
DISC
28

Four steps to ignition

Commission laser

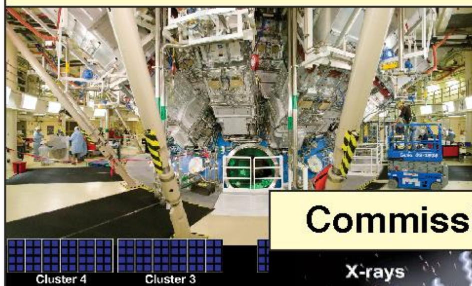

Commission hohlraum

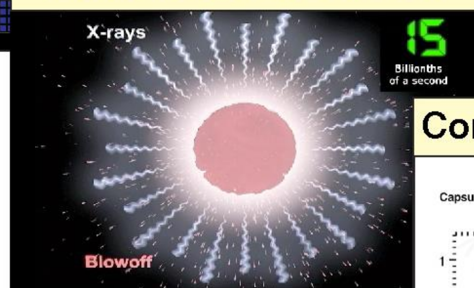

Commission capsule

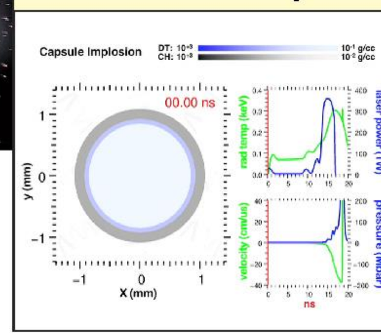

Commission layered target implosions

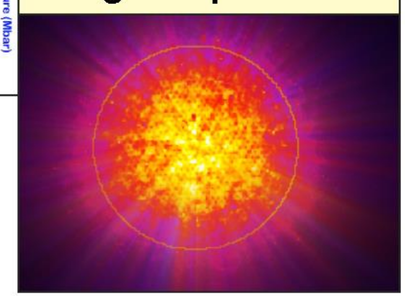

We are taking a systematic approach to learning and improving our enginering design to achieve ignition

Highlights of progress towards ignition

Commission laser

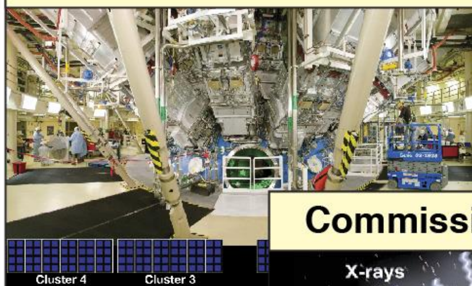

1.855 MJ
523 TW
300:1 contrast

Commission hohlraum

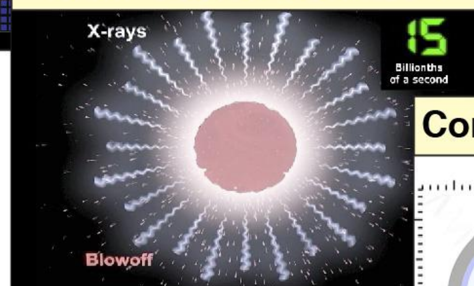

330 eV
~85% absorbed energy

Commission capsule

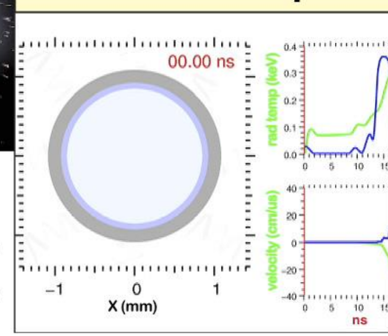

Convergence ratio ~35,
ρR ~1.3 gm/cm^2 (85% of requirement)
$V_{implosion}$ ~350 km/sec

Commission layered target implosions

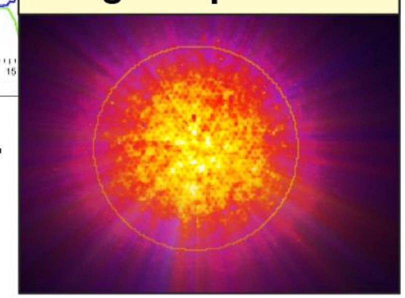

Pressure ~150 GBar

Y~9e14

Highlights of progress towards ignition

Commission laser

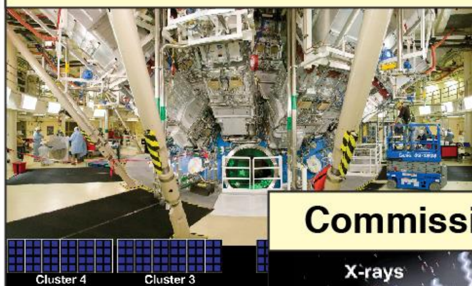

1.855 MJ
523 TW
300:1 contrast

Commission hohlraum

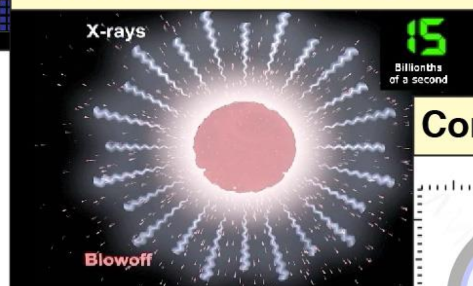

330 eV
~85% absorbed energy

Commission capsule

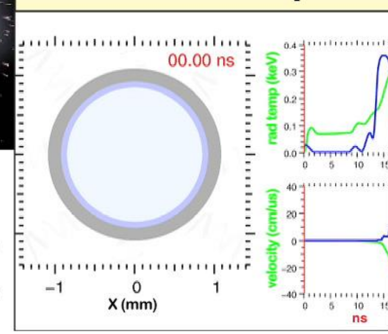

Convergence ratio ~35,
ρR ~1.3 gm/cm² (85% of requirement)
$V_{implosion}$ ~350 km/sec

Commission layered target implosions

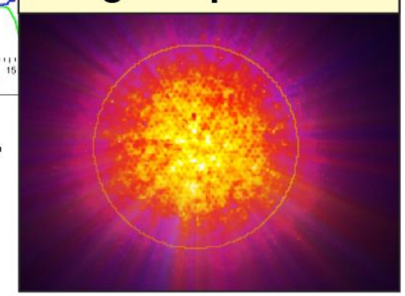

?

Pressure ~150 GBar

Y~9e14

We have made good progress towards achieving ignition conditions on the NIF

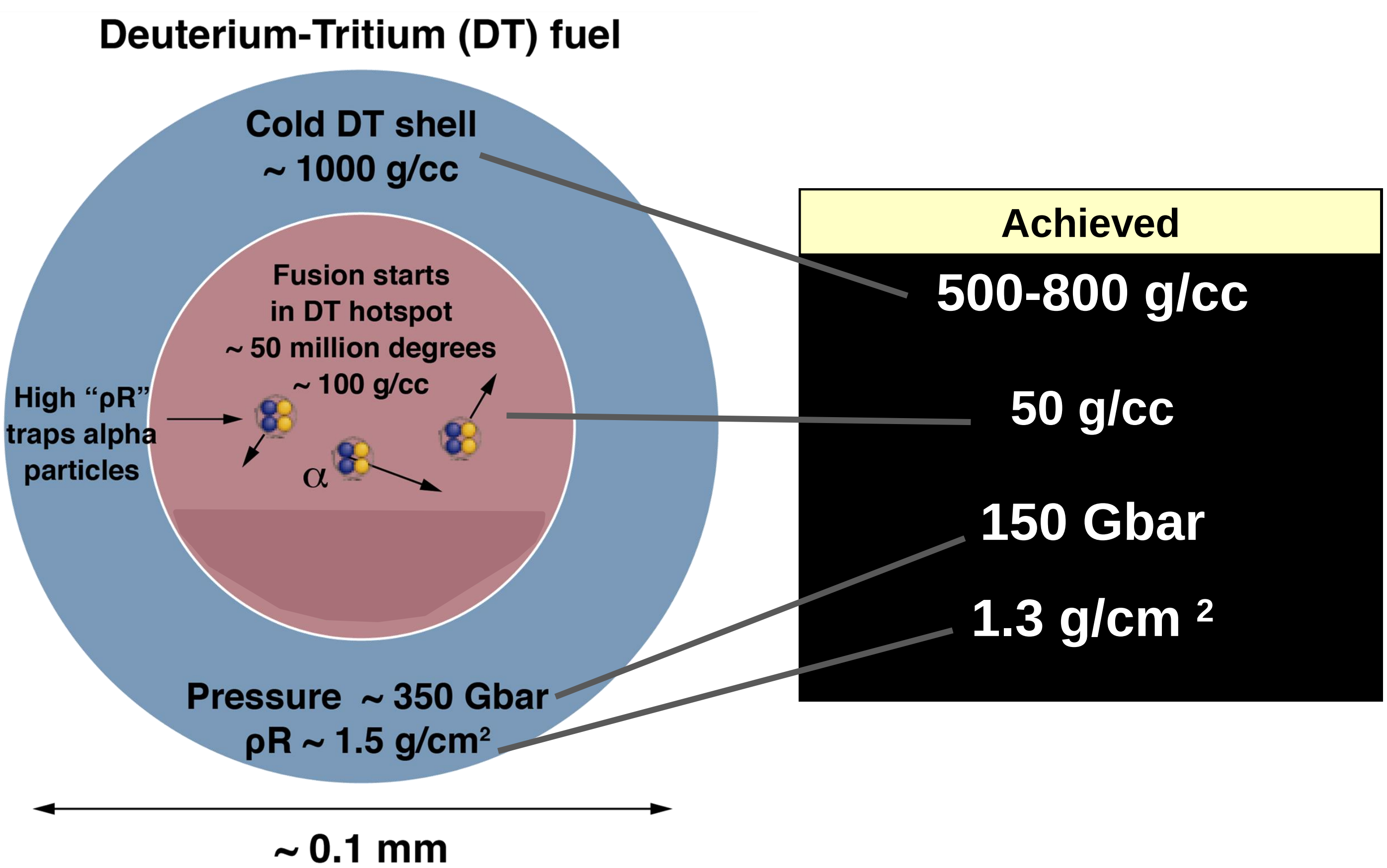

32

Hohlraum physics- fraction of laser energy coupled is ~ 85%, and drive scales as expected

Laser-hohlraum coupled energy

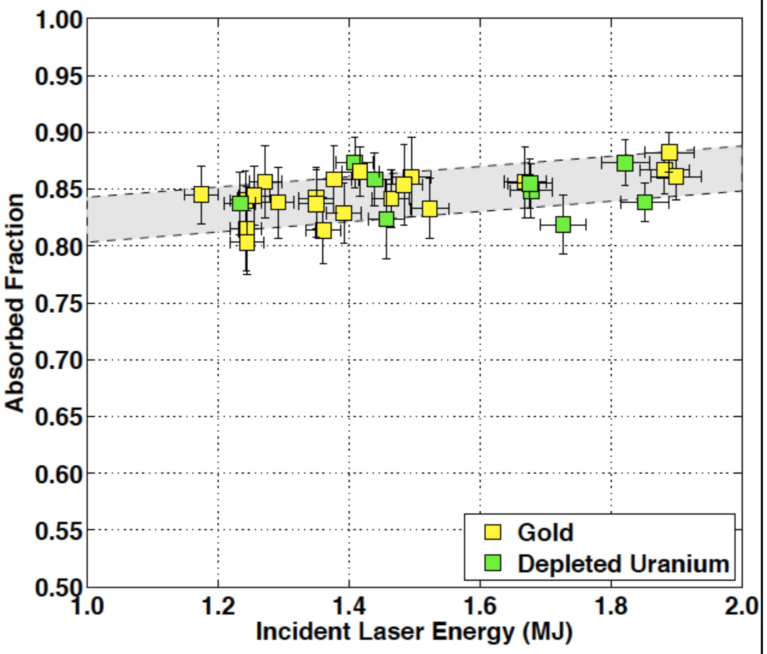

Hohlraum drive vs laser energy

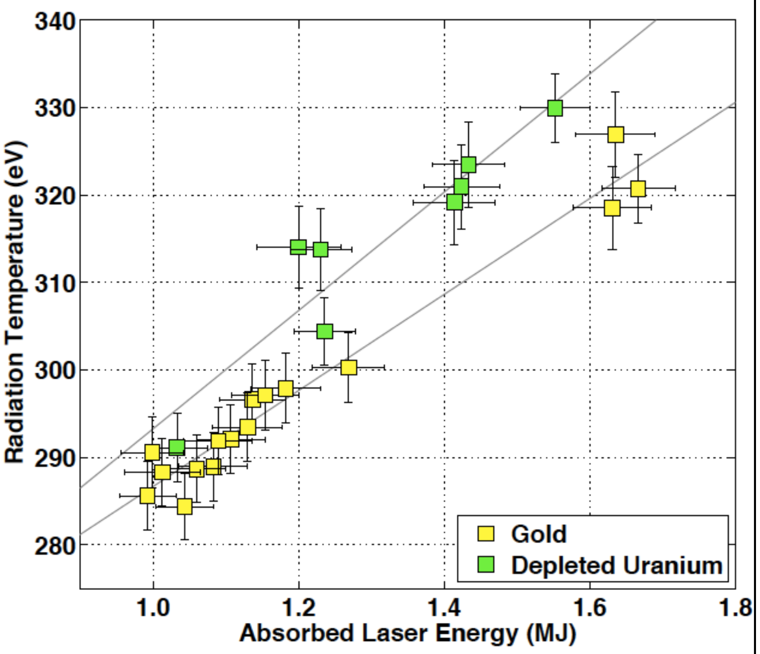

Pressure and velocity in cryogenic layered implosions is approaching conditions required for ignition

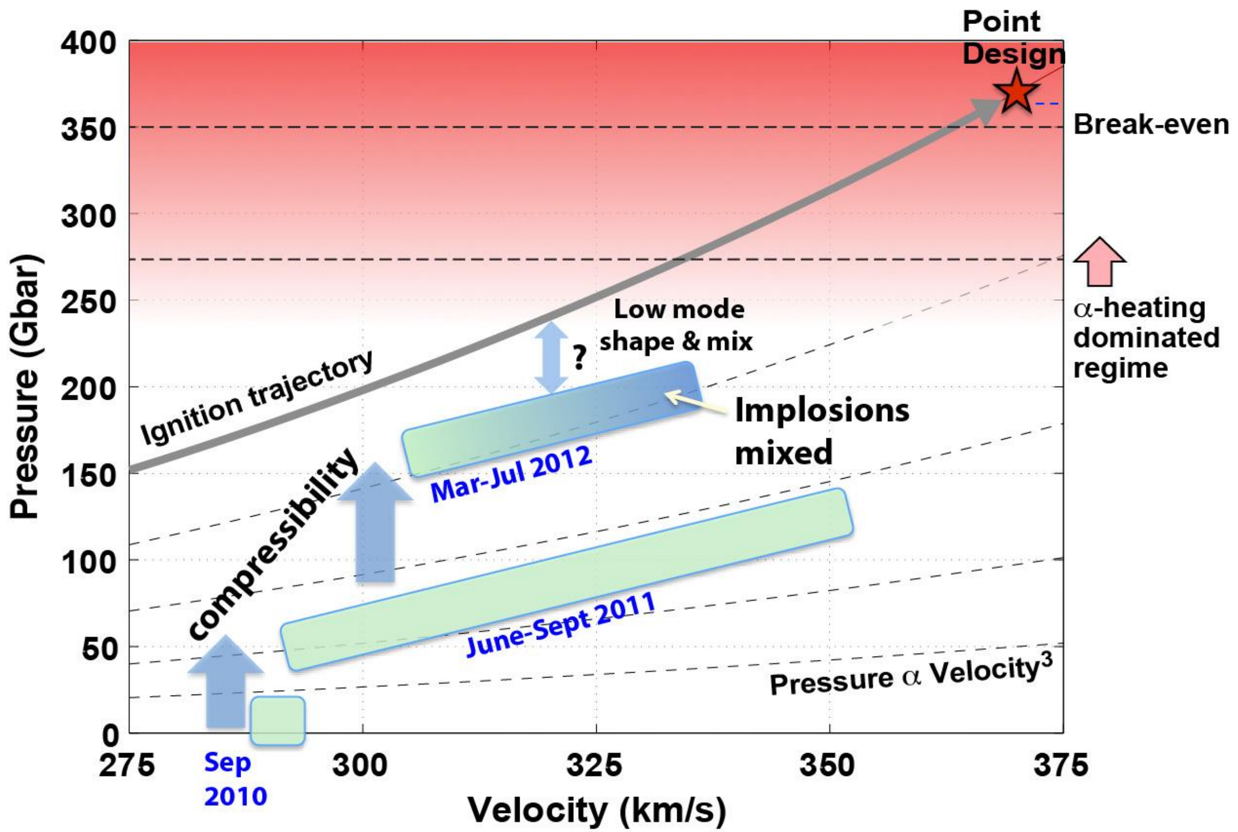

The capsule starts at 2mm diameter

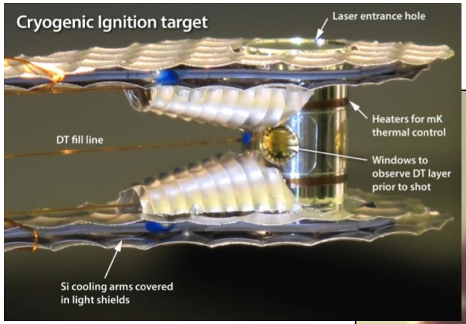

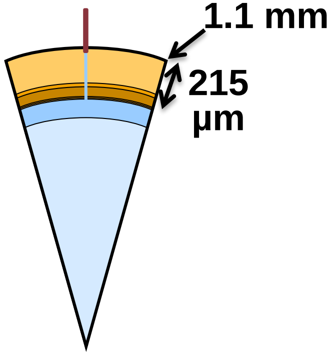

~2 mm

2013-049951s2.ppt

35

The hot spot viewed in x-ray emission looks quite round

DT shot N120716
Bang time

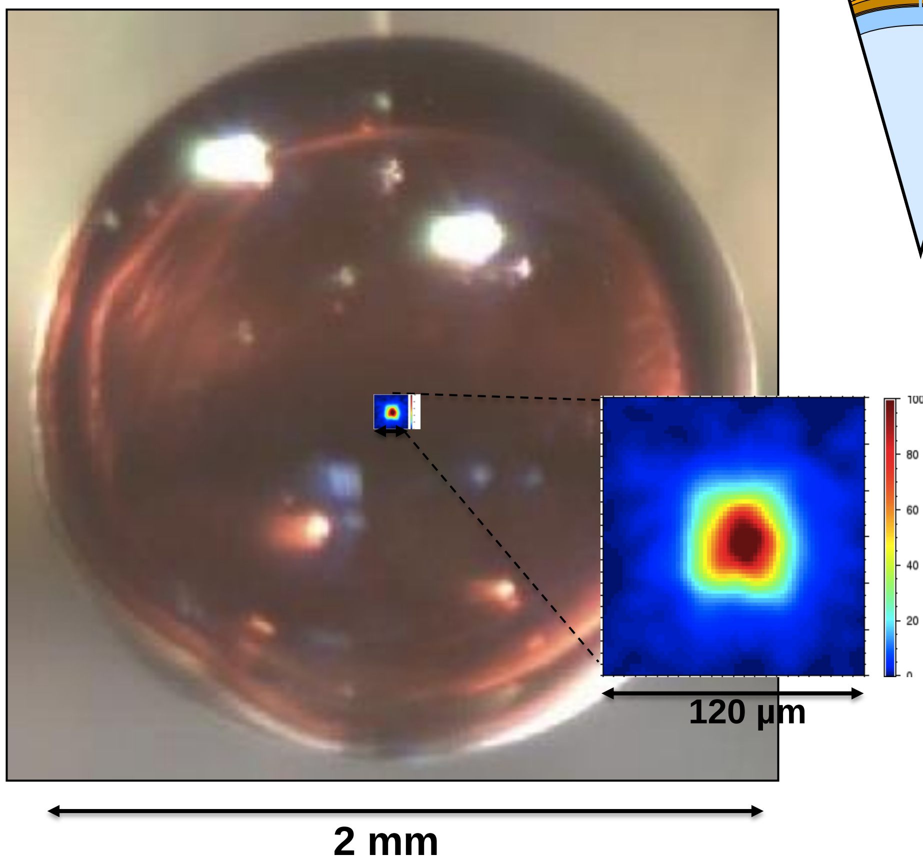

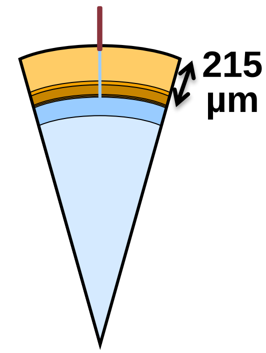

P4 “diamond” shape clearly seen during the implosion

N121004

Bang time – 600ps

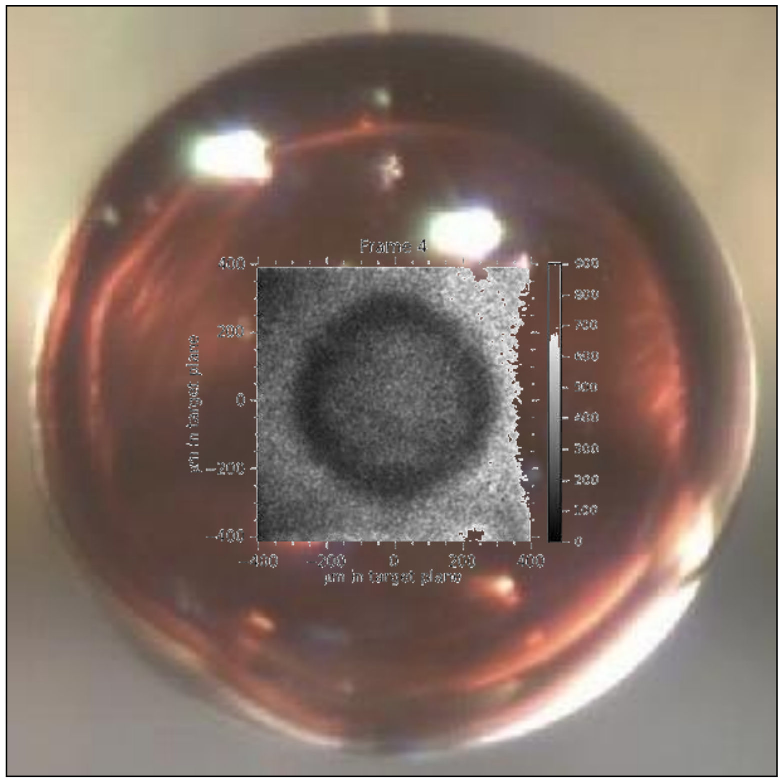

~2 mm

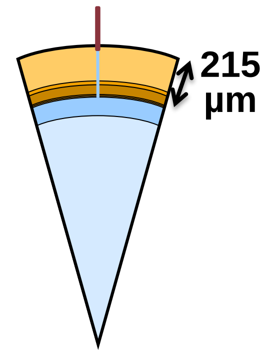

P4 "diamond" shape clearly seen during the implosion

N121004

Bang time – 300ps

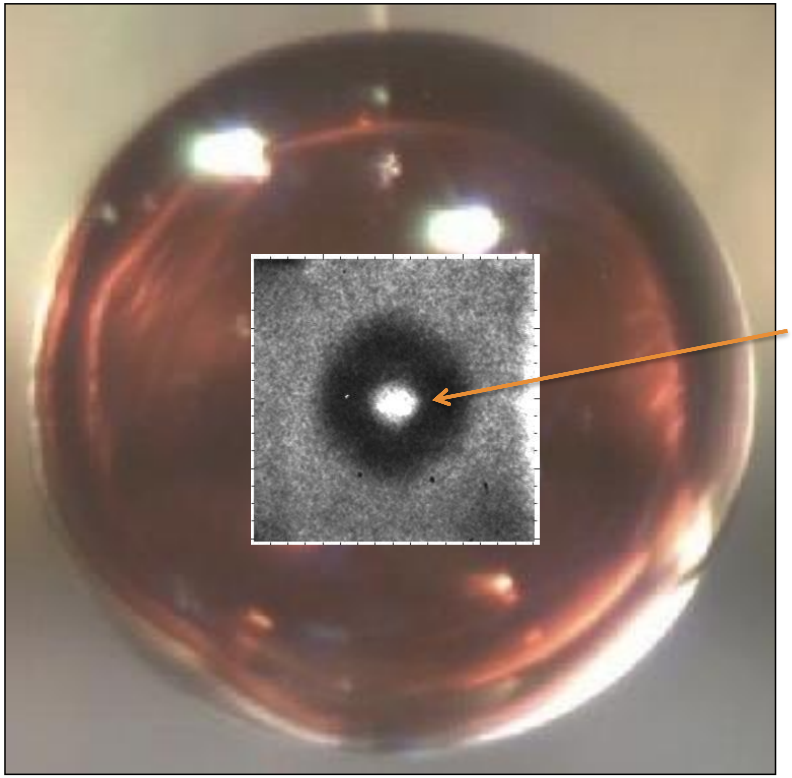

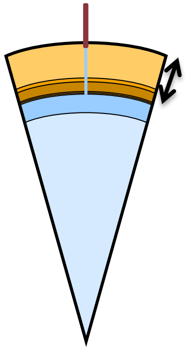

Early hot spot formation

~2 mm

Compton radiography for stagnated fuel: Promising results but improvements needed

N121005
Bang time

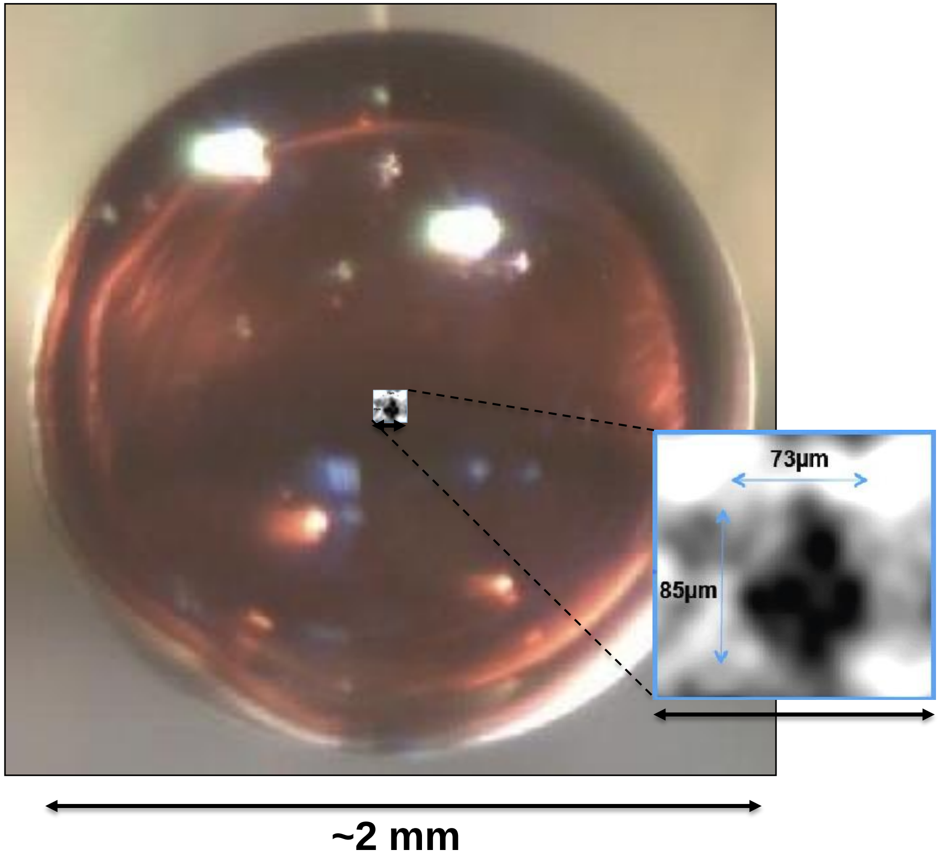

Preliminary analysis

Significant fuel ρR asymmetry measured by neutron activation detectors (FNADS)

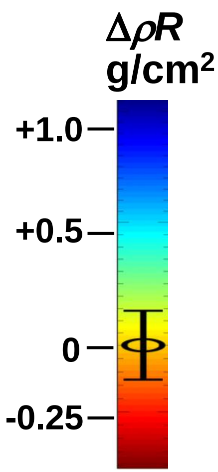

ρR map from neutron Activation Detectors
($^{90}Zr(n,2n) \Rightarrow {}^{89}Zr$)

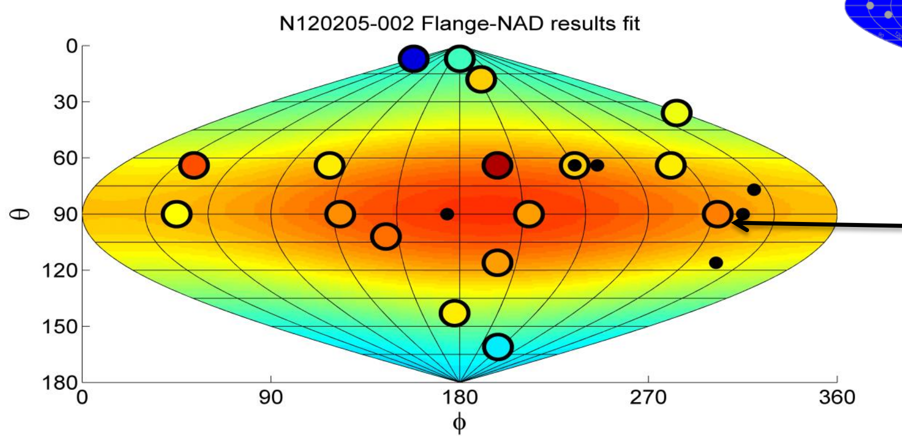

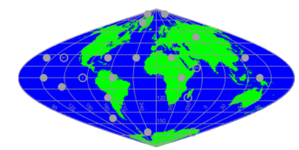

- Average ρR ~ 1 g/cm^2
- ~ 50% variations

Motivates new 2D backlit imaging of the implosion
Motivates Compton radiography for stagnated fuel shape

NIF Advanced Radiographic Capability (ARC) is needed to diagnose evolution of cold fuel shape

Predicted synthetic images of stagnated DT fuel
Requires 50-100 keV X-rays

3w NIF without ARC | **ARC**

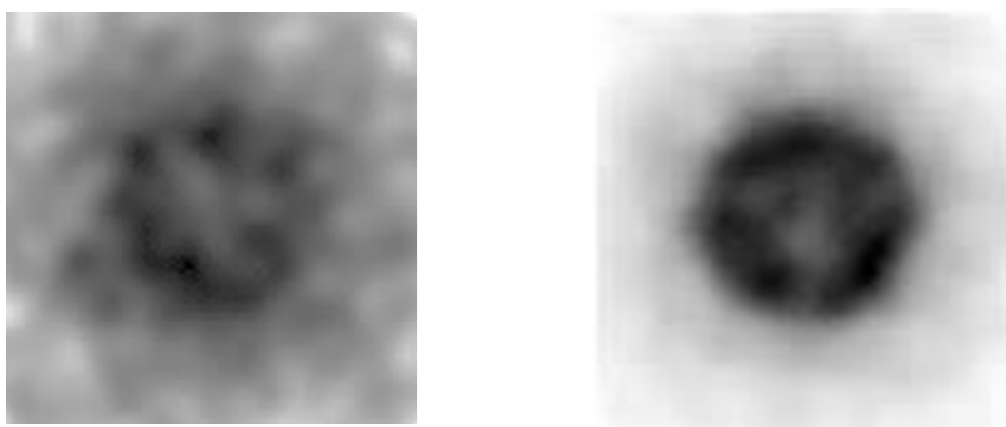

~ 100 µm

ARC estimated accuracy in fuel ρR ~ 5-10% over ~ 10µm resolution element

Yield correlates strongly with hot spot mix-ablation front instability growth appears to be the issue

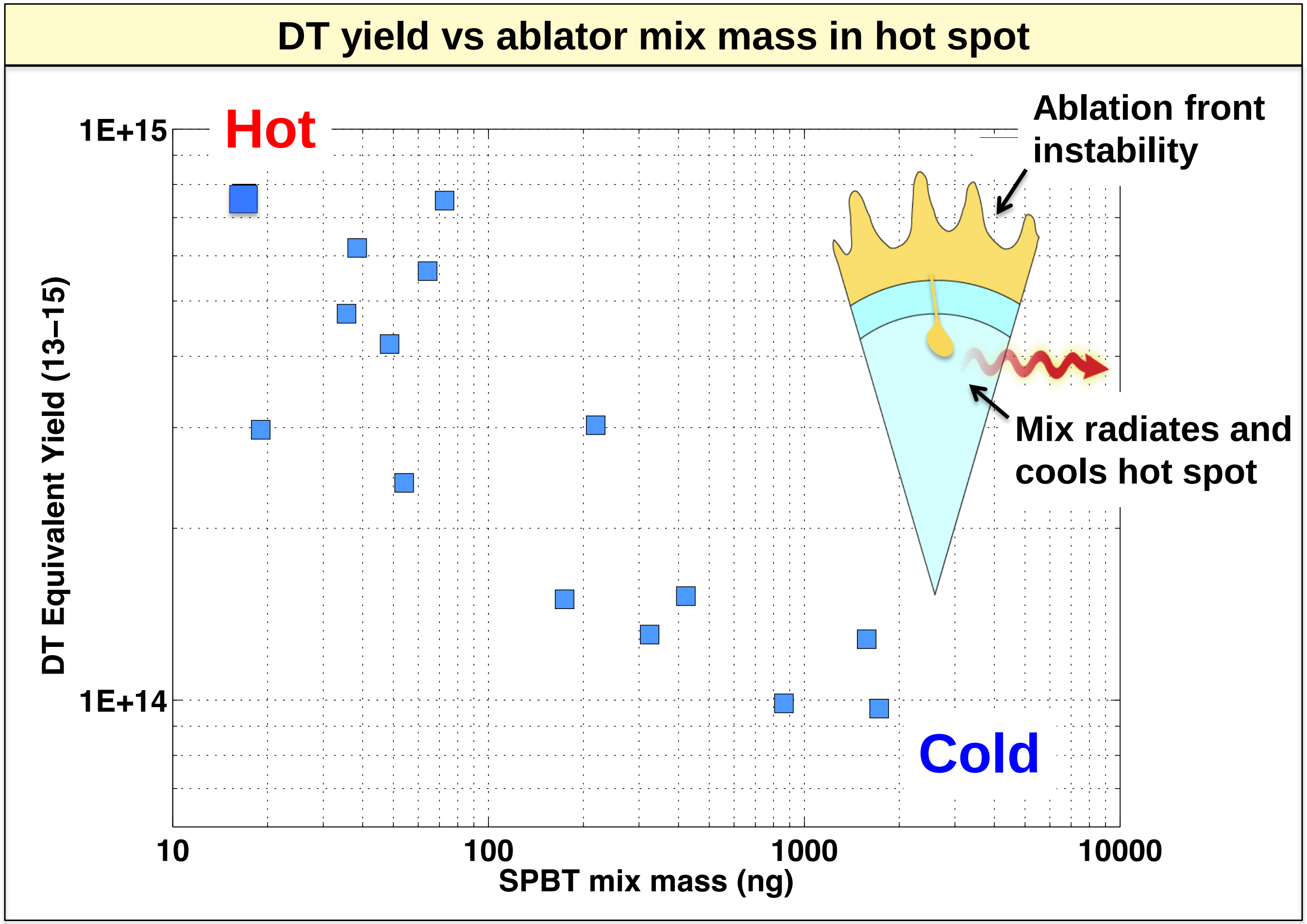

The principal issues on ignition performance deficit

Fuel shape

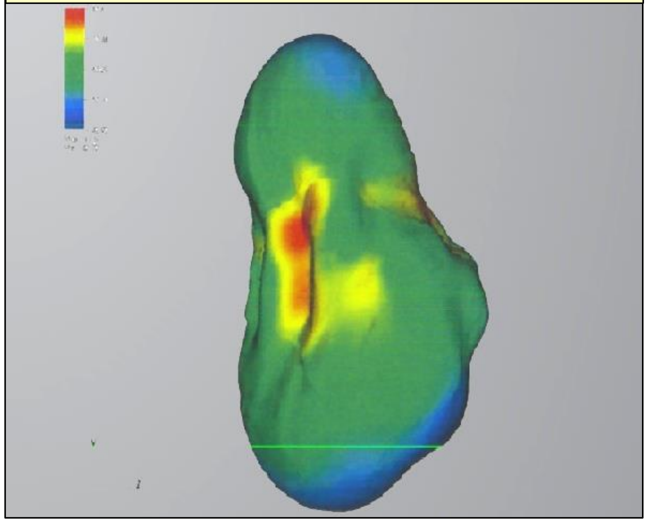

Mix

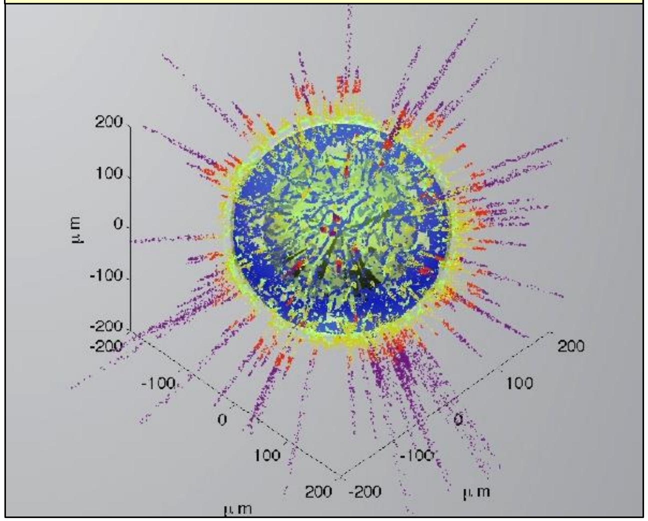

- **Performance deficit likely due to combination of low mode X-ray drive asymmetry/cold fuel shape, and higher than simulated hydrodynamic instability**

Identifying the reasons for the deficit in pressure/performance and developing mitigation strategies is a key element of the go-forward experimental plan

NIF continues to make good progress towards achieving the conditions necessary for ignition

- The NIF laser and targets have met the highly demanding specifications for accuracy and control required by the ignition point design (Rev5)
- The hohlraum X-ray drive exceeded the ignition goal of 300eV accelerating implosions up to ~ 350 km/s (goal 370 km/s)
- Fuel ρR up to 1.3 g/cm^2 were achieved (1.5 g/cm^2 goal)
- Nuclear yields are ~ 3-10X from alpha dominated regime
  - — hotspot densities, pressures are ~ 2-3X lower than predicted/required
- Performance deficit likely due to combination of low mode X-ray drive asymmetry/cold fuel shape, and higher than simulated hydrodynamic instability

Good progress is being made in developing new experimental capabilities to identify the key reasons for the deficit in hot spot density, pressure and yield

Recent data show that P4 asymmetry can be modified by extending the hohlraum length

P4 shape at ~ 200 µm vs. hohlraum length

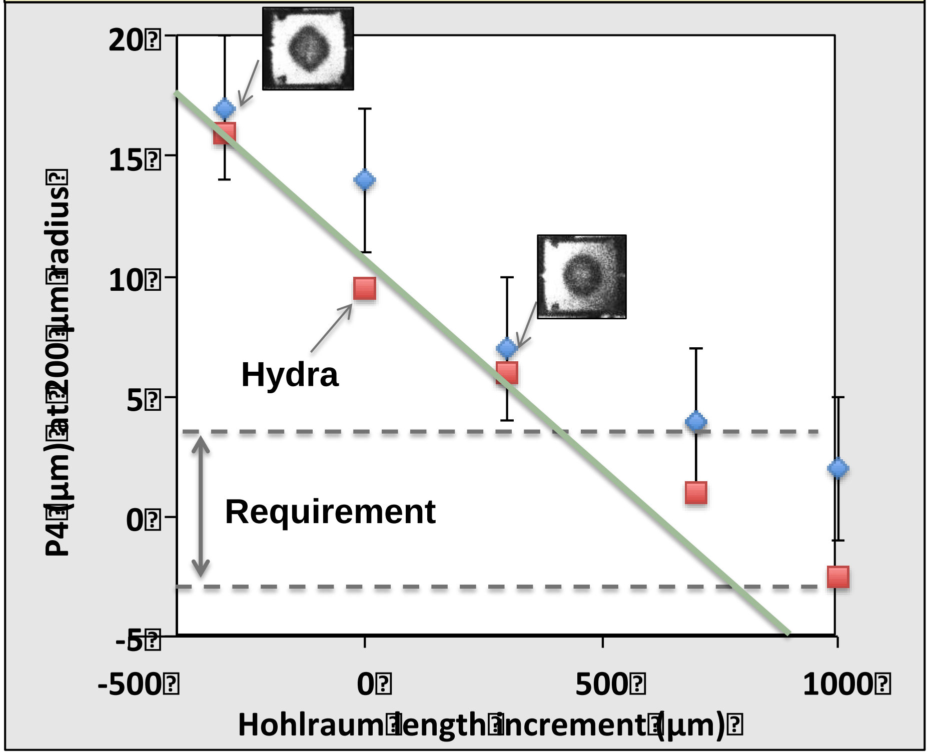

Time dependence of P4 symmetry remains an important question

Higher adiabat DT layered implosion performs closer to 1D

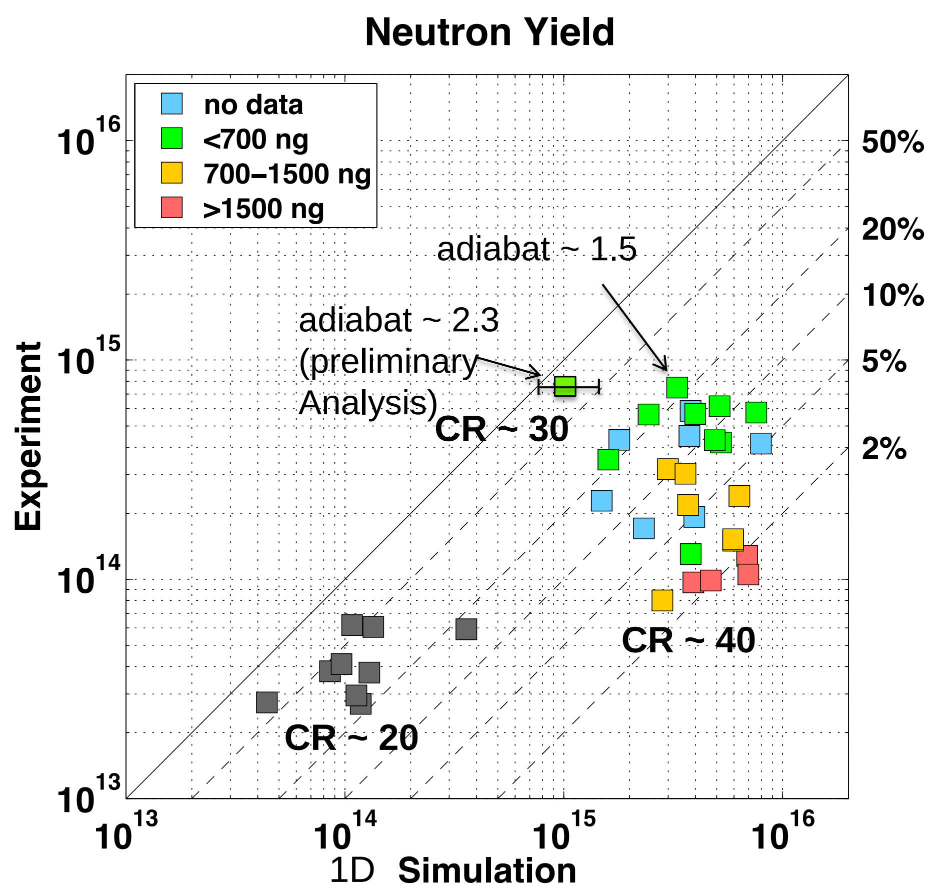

The principal issues and go-forward strategy were summarized in a Dec. 2012 NNSA report to Congress and the Science of Fusion Ignition Workshop Report

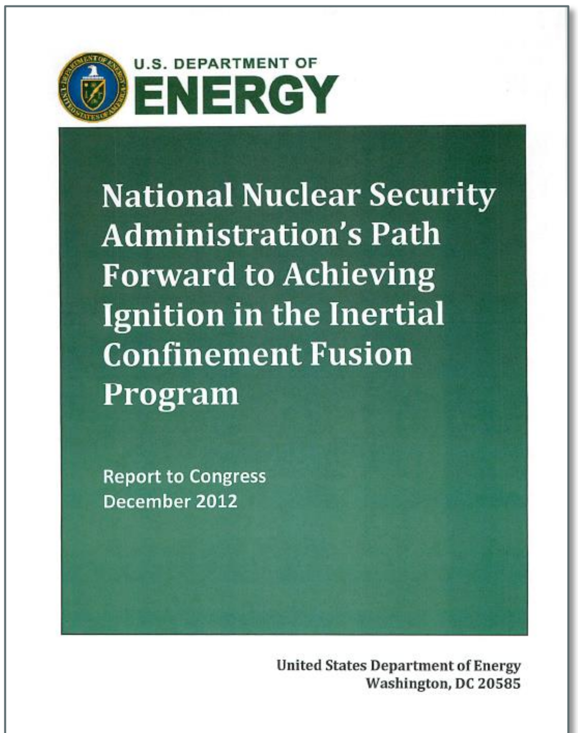

We welcome and encourage the broader scientific community to engage In the ignition science program

Fundamental science on NIF was addressed most recently in a 2011 NNSA/Office of Science report

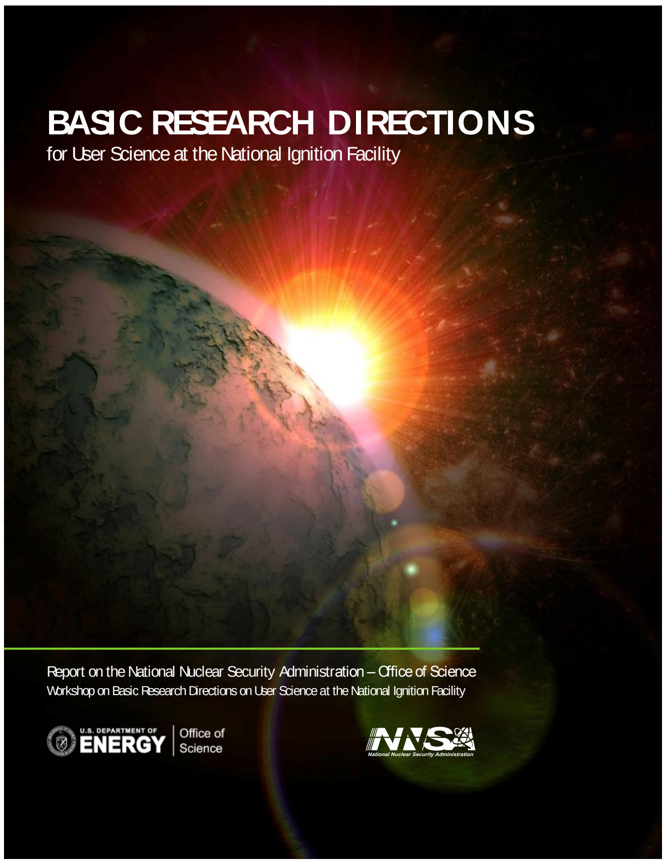

Summary of Workshop Priority Research Directions	
Panels	**Priority Research Directions**
1. Laboratory Astrophysics	1.1 Simulating Astrochemistry: The Origins and Evolution of Interstellar Dust and Prebiotic Molecules
	1.2 Explanation for the Ubiquity and Properties of Cosmic Magnetic Fields and the Origin of Cosmic Rays
	1.3 Radiative Hydrodynamics of Stellar Birth and Explosive Stellar Death
	1.4 Atomic Physics of Ionized Plasmas
2. Nuclear Physics	2.1 Stellar and Big Bang Nucleosynthesis in Plasma Environments
	2.2 Formation of the Heavy Elements and Role of Reactions on Excited Nuclear States
	2.3 Atomic Physics of Ionized Plasmas
3. Materials at Extremes and Planetary Physics	3.1 Quantum Matter to Star Matter
	3.2 Elements at Atomic Pressures
	3.3 Kilovolt Chemistry
	3.4 Pathways to Extreme States
	3.5 Exploring Planets at NIF
4. Beams and Plasma Physics	4.1 Formation of and Particle Acceleration in Collisionless Shocks
	4.2 Active Control of the Flow of Radiation and Particles in HEDP
	4.3 Ultraintense Beam Generation and Transport in HED Plasma
	4.4 Complex Plasma States in Extreme Laser Fields

NIF fundamental science program started in FY2009 via existing collaborations

Equation of state/planetary interiors (UC Berkeley, Princeton, LLNL)

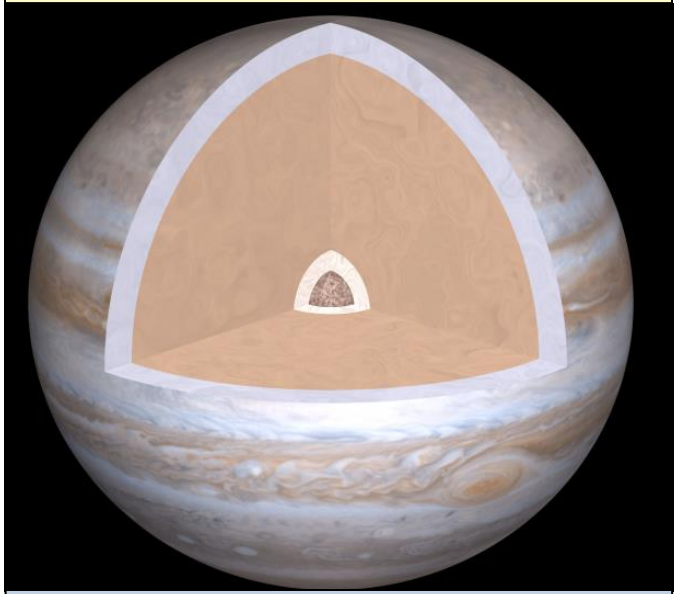

Examine EOS of compressed diamond, iron at pressures up to 50-100 MBar

Supernova hydrodynamics-radiative effects (Univ. of Michigan, LLNL)

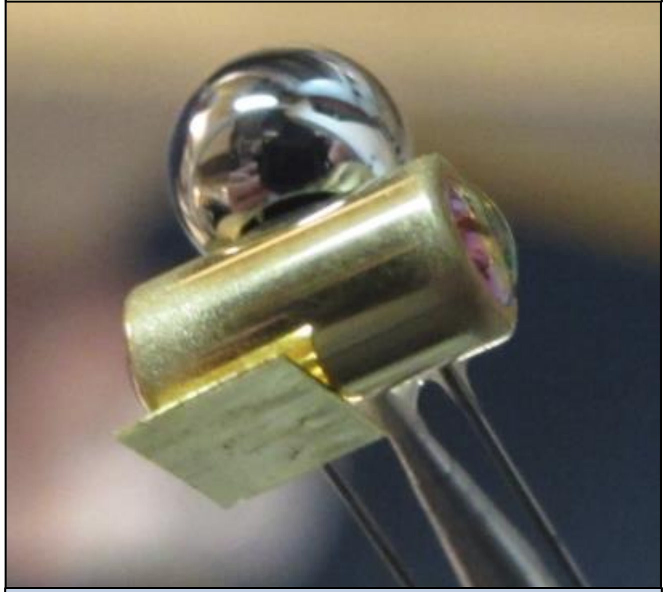

Examine effects of radiation on growth of Rayleigh-Taylor instability

NIF has been used to “shocklessly” compress carbon to 50 Mbar

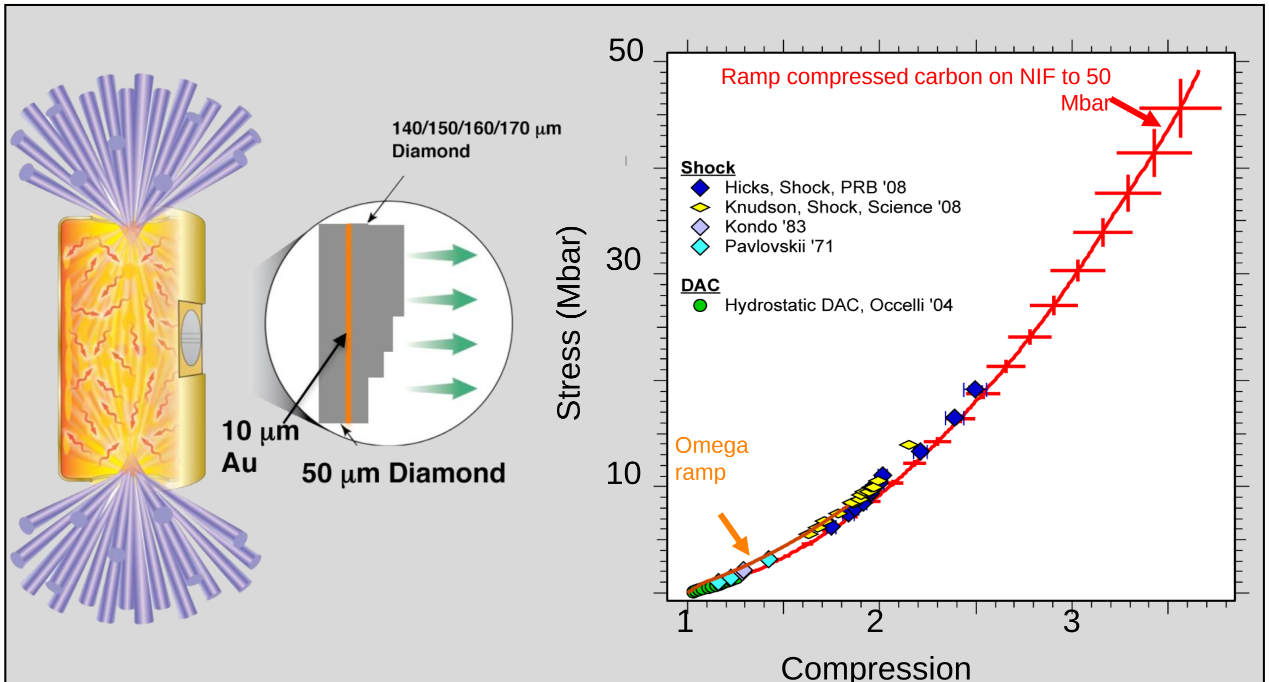

R.F. Smith, J.H. Eggert, D.G. Braun, J.R. Patterson-1, R.E. Rudd, R. Jeanloz, T.S. Duffy, J. Biener, A.E.Lazicki, A.V. Hamza, J. Wang, T. Braun, L.X. Benedict, P.M. Celliers, G.W. Collins

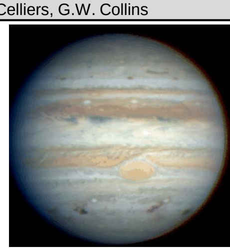

NIF can now recreate the most extreme planetary core states in the solar system

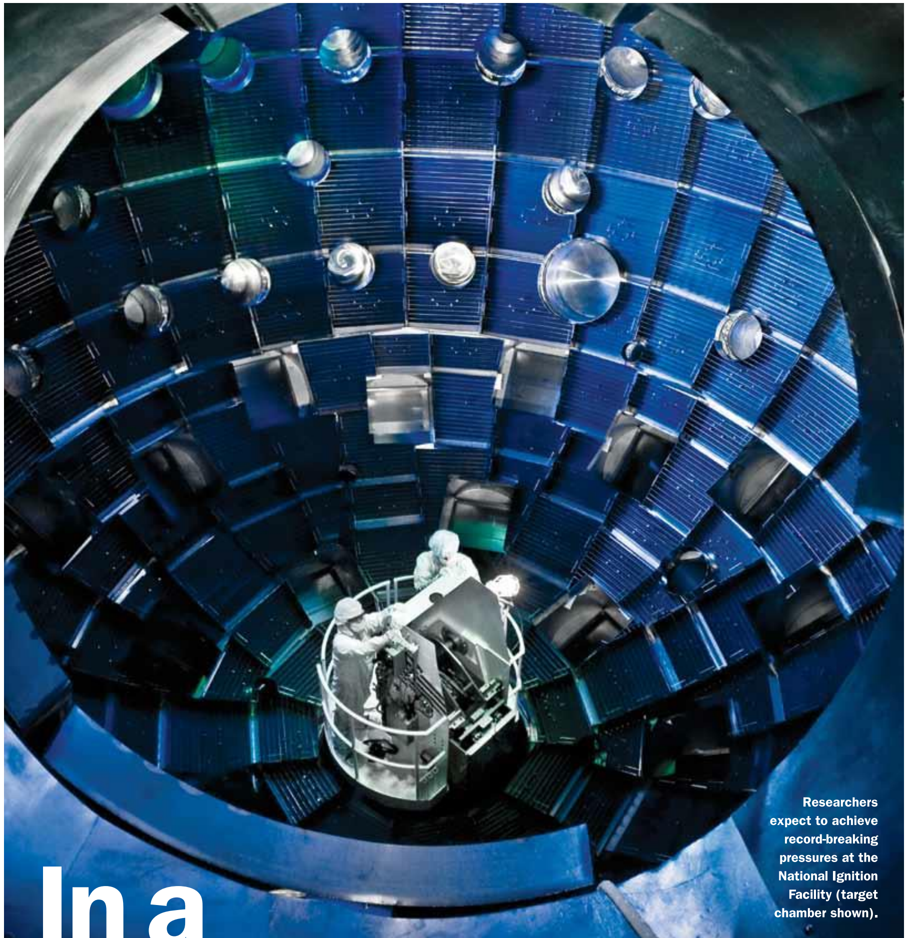

Researchers expect to achieve record-breaking pressures at the National Ignition Facility (target chamber shown).

In a SQUEEZE

Elements under pressure reveal secrets of extreme chemistry

By Alexandra Witze

Bruce Banner isn't the only scientist who could crush you with one mighty squeeze. These days, the Hulk's superhuman strength is matched by researchers who squish all kinds of stuff in superscience experiments.

The goal isn't to save the world from baddies, but to explore new frontiers in the nature of matter. After all, most material in the universe exists at bone-crushing pressures. Think massive stars and planetary cores — realms no comic book fan or other Earth dweller has ever seen.

Deep within the planet, rock experiences pressures more than 1 million times as great as the "1 atmosphere" that ordinary humans live under at sea level. Pressures at the centers of ultradense neutron stars are some trillion quadrillion times greater. Under such extreme conditions, atoms themselves begin to buckle.

To mimic these hellish realms, scientists are ramping up pressure in the lab, like the Hulk getting ever stronger as he gets madder. In the process, they're squeezing out some surprising insights.

One team has found a new kind of iron oxide, a compound that somehow had never been seen before, even though it contains two of the most common elements in Earth's crust. Another group argues that hydrogen's odd behavior at high pressures means that the cores of giant gas planets, such as Jupiter, are eroding in a slow hydrogen drip. Meanwhile scientists at the National Ignition Facility in Livermore, Calif., have squeezed diamond to record pressures, uncovering unexpected and exotic behaviors.

Chemistry, it seems, is a different beast under high pressure. "We're developing a whole new paradigm for understand-

FACING PAGE: LAWRENCE LIVERMORE NATIONAL LABORATORY; THIS PAGE: T. DUBÉ

"Meanwhile scientists at the National Ignition Facility in Livermore, Calif., have squeezed diamond to record pressures, uncovering unexpected and exotic behaviors."

NIF issued a call for proposals for fundamental science experiments in FY2010

FY2010 Call for Proposals

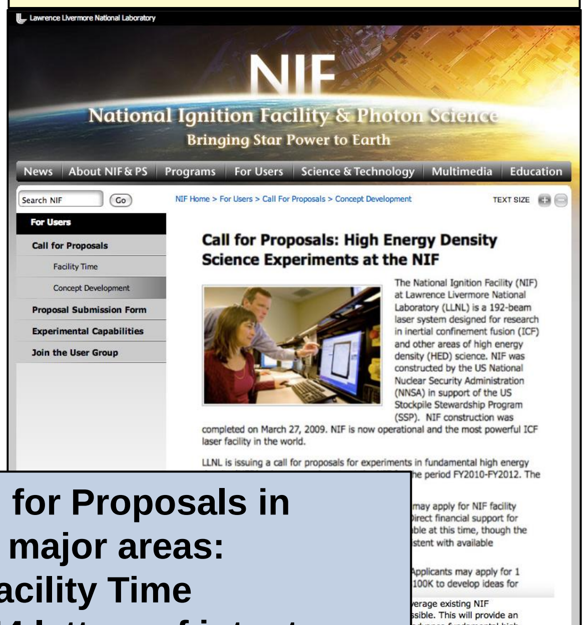

NIF Science Technical Review Committee (TRC) (R. Rosner, Chair)

Call for Proposals in two major areas:

- **Facility Time (44 letters of intent, 40 full proposals)**
- **Concept Development ($100k maximum 1 year awards, 42 proposals)**

NIF fundamental science call was the first general proposal issued by NIF and provided valuable insight and experience for implementing NIF governance in support of all missions

Proposals selected in FY2010 call span an exciting spectrum of scientific questions

Observing new states of matter (H)

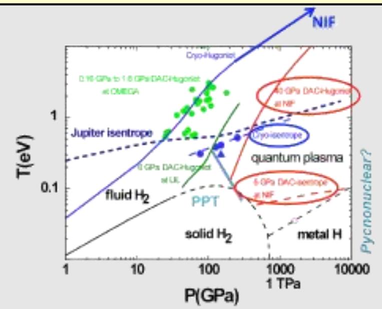

UC Berkeley, Carnegie Institution

Understanding the most energetic events in the universe

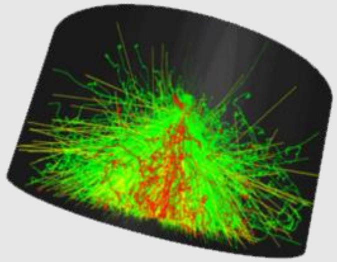

LLNL

How do supernovae Explode?

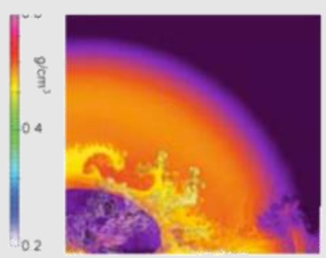

Florida State University

Probing the highest energy density states on Earth

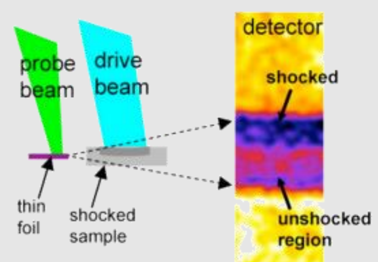

GSI/UC Berkeley

Proposals selected in FY2010 call span an exciting spectrum of scientific questions (cont.)

Origin of ultra-high energy cosmic rays

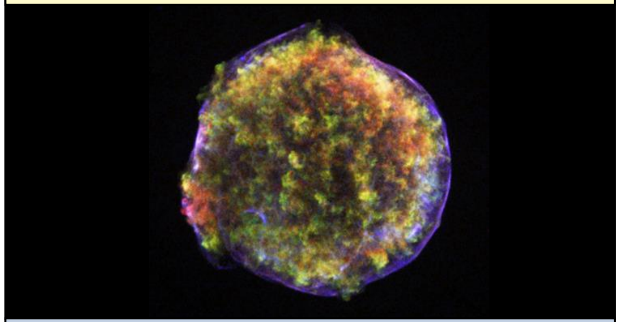

Osaka Univ./Oxford Univ.

Large-scale behavior of matter in the universe

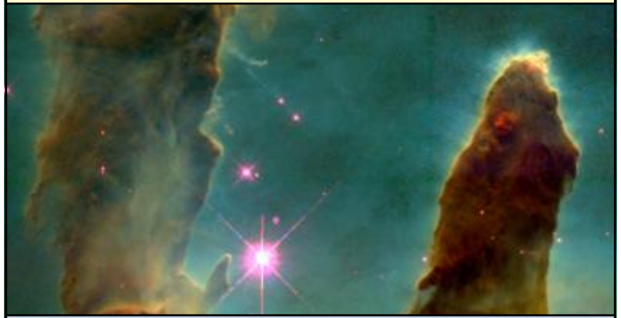

CEA/LLNL

Synthesis of elements heavier than iron

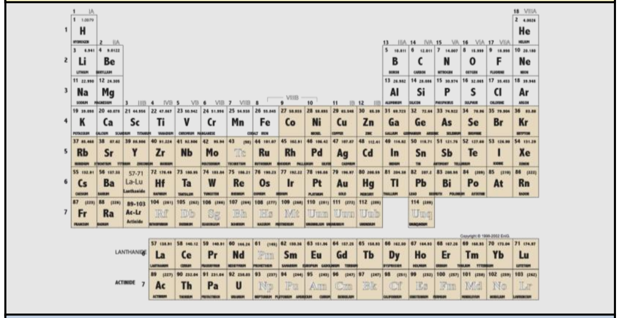

LLNL

Novel phases of compressed diamond

Oxford Univ./LLNL

The high *e*, γ and n-flux in a NIF capsule might allow us to explore reactions on short-lived nuclear states

Neutron flux in NIF imploded capsules is comparable to supernovae

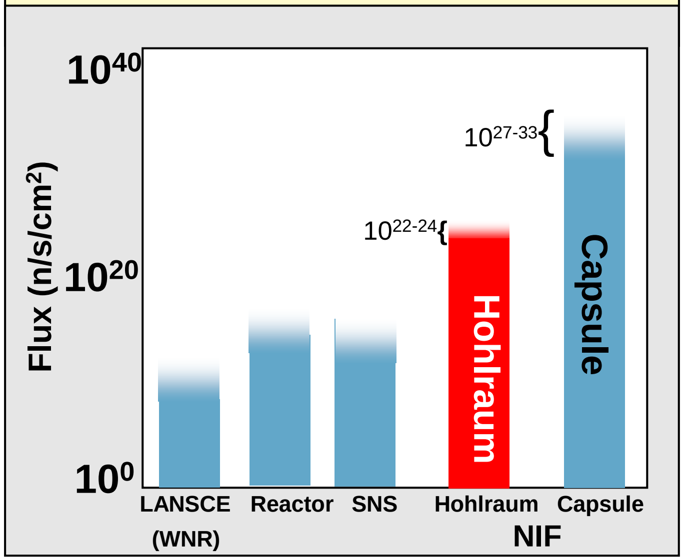

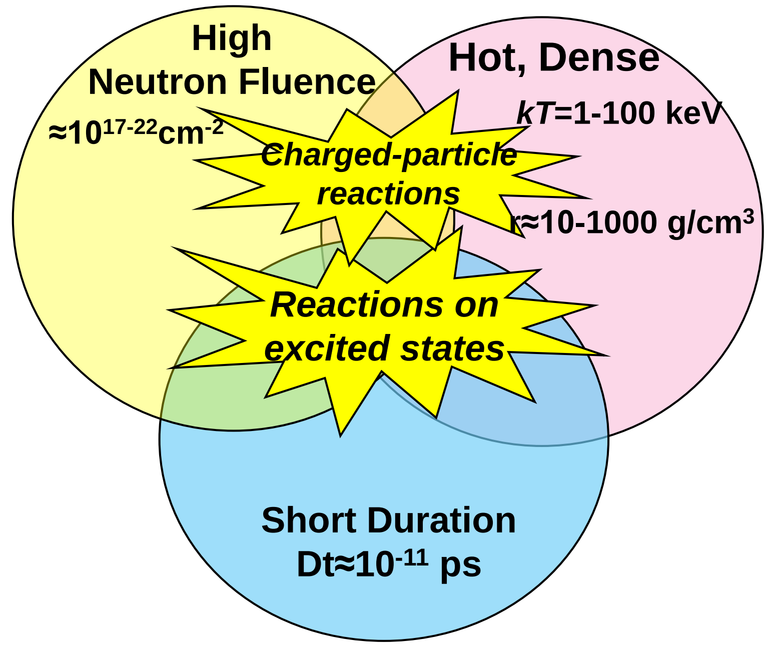

The NIF nuclear diagnostic team has obtained data from 58 “ride-along” experiments

Production of low energy neutrons in ICF implosions is important for nuclear cross sections for astrophysics and ICF ρR_{fuel} diagnostics

Four collectors mounted on a DIM

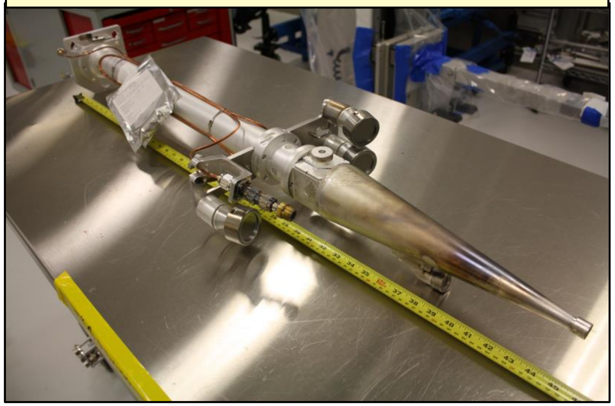

^{198}Au produced by downscattered neutrons-γs counted in B151

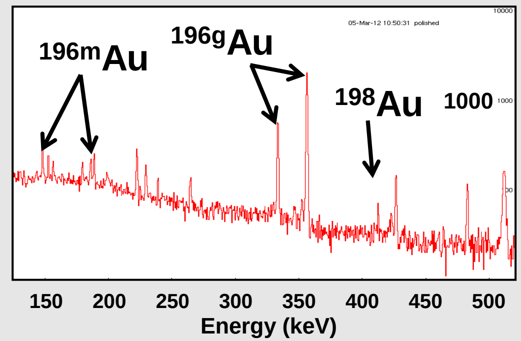

Inferred low-energy neutron spectrum similar to that of stars

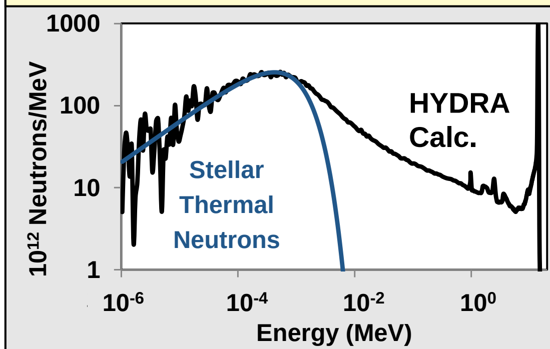

^{198}Au/^{196}Au is also a ρR_{fuel} diagnostic

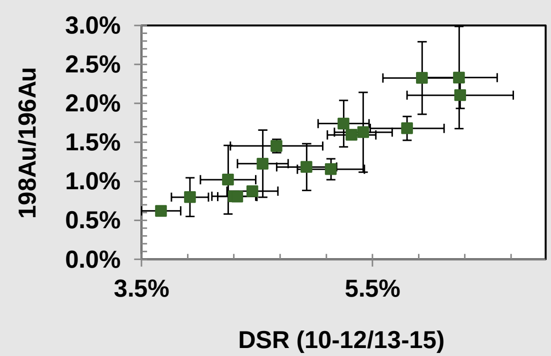

The NIF NTOF-20 system has for the first time observed the sequential decay of the T+T system in a HED plasma

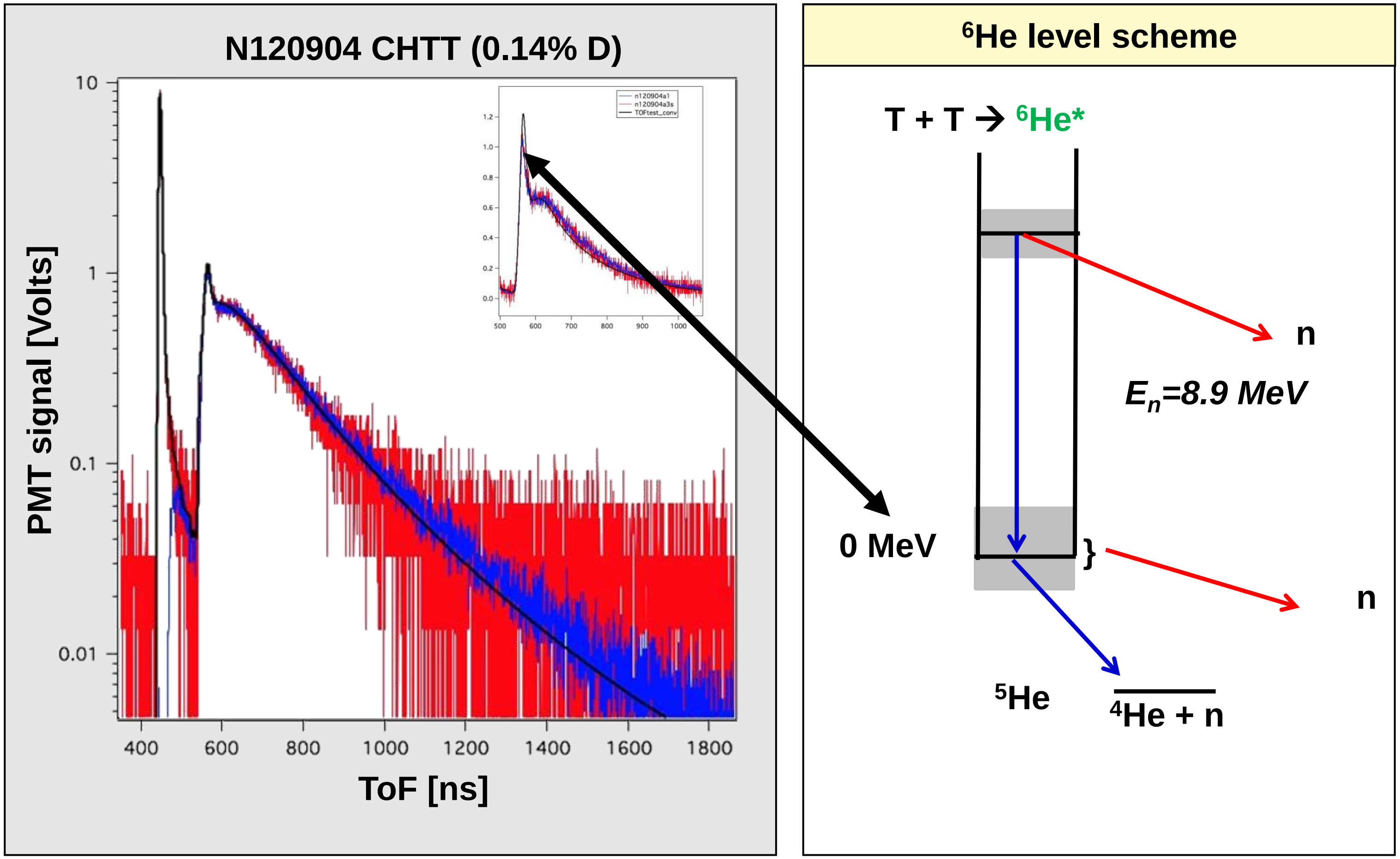

A tantalizing result: can we observe plasma effects on excited state populations?

R= ^{196m}Au (J=12) /^{196g}Au (J=2) greater on equator vs. pole

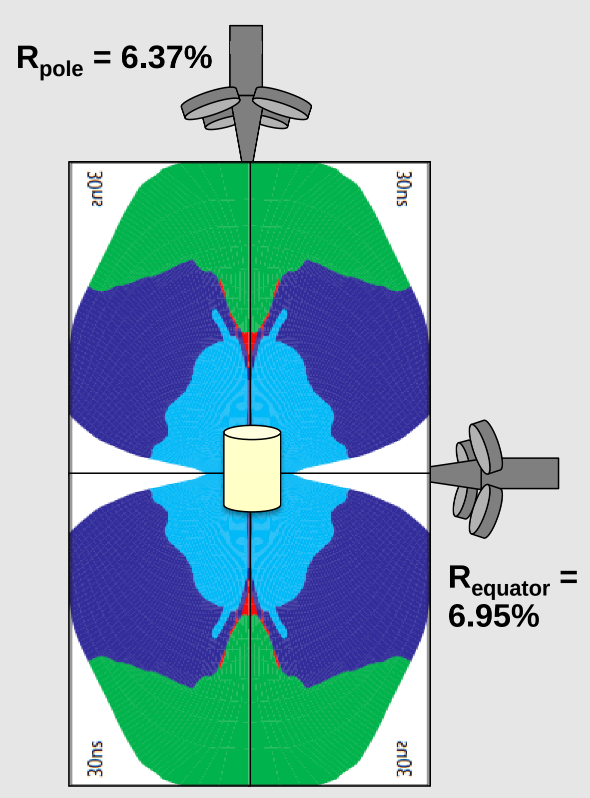

Direct drive experiments with ^{134}Xe proposed

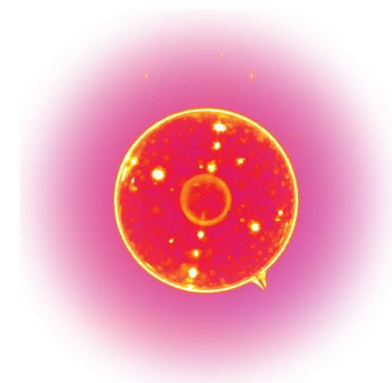

The first LLNL-CEA ablative Rayleigh-Taylor experiment was conducted on March 21, 2013

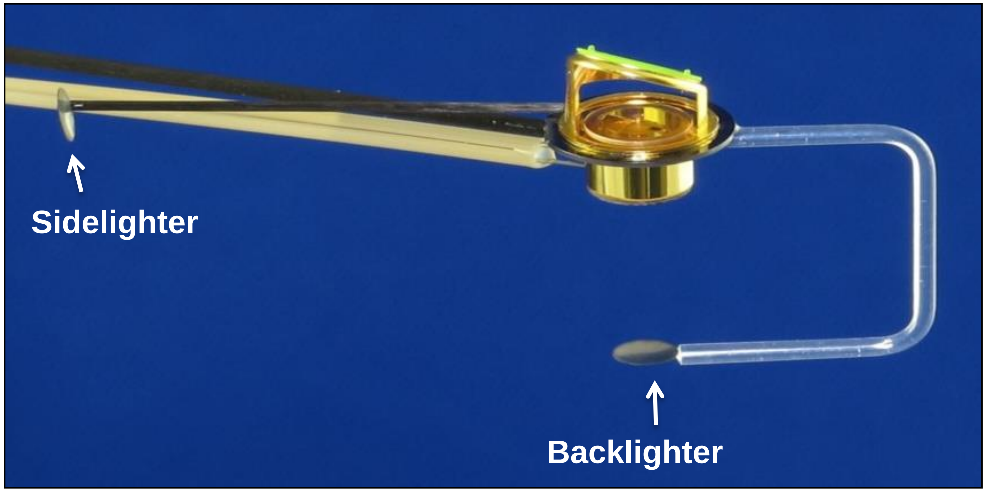

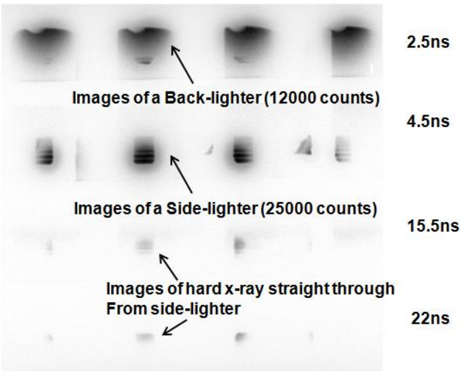

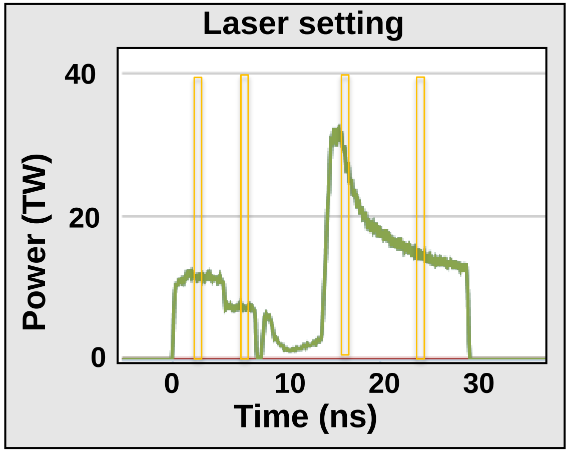

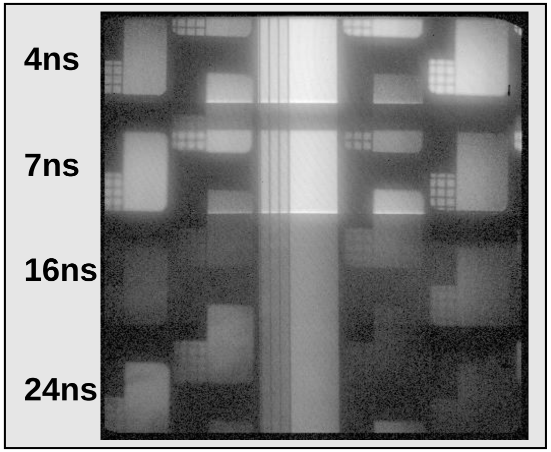

- **Hohlraum background and backlighter signal level verified to be adequate**

NIF collisionless shock experiment under development builds on results from Omega showing unexpected self-organizing stable field structures

Images obtained at Omega via proton radiography

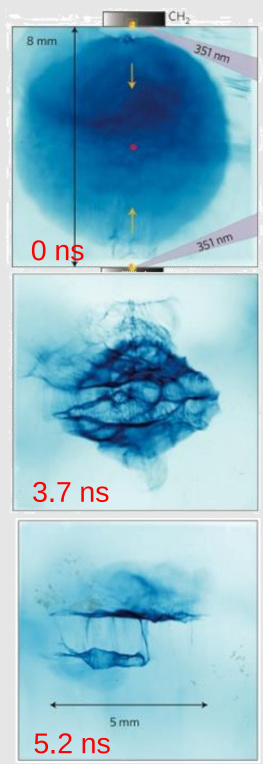

N. Kugland et al., Nature Physics (2012)

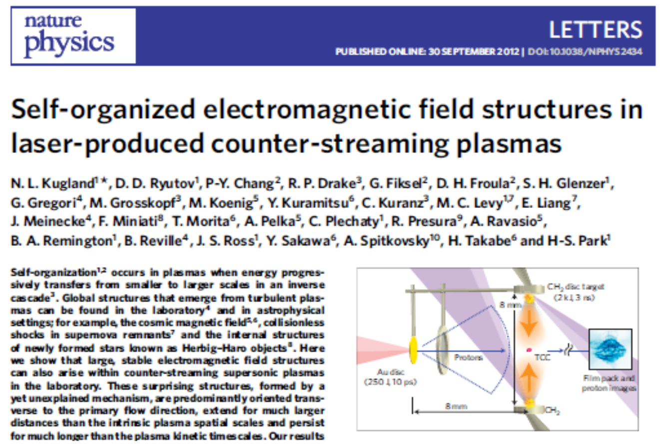

nature physics

LETTERS

PUBLISHED ONLINE: 30 SEPTEMBER 2012 | DOI: 10.1038/NPHYS2434

Self-organized electromagnetic field structures in laser-produced counter-streaming plasmas

N. L. Kugland[1]*, D. D. Ryutov[1], P-Y. Chang[2], R. P. Drake[3], G. Fiksel[2], D. H. Froula[2], S. H. Glenzer[1], G. Gregori[4], M. Grosskopf[3], M. Koenig[5], Y. Kuramitsu[6], C. Kuranz[3], M. C. Levy[1,7], E. Liang[7], J. Meinecke[4], F. Miniati[8], T. Morita[6], A. Pelka[5], C. Plechaty[1], R. Presura[9], A. Ravasio[5], B. A. Remington[1], B. Reville[4], J. S. Ross[1], Y. Sakawa[6], A. Spitkovsky[10], H. Takabe[6] and H-S. Park[1]

Self-organization[1,2] occurs in plasmas when energy progressively transfers from smaller to larger scales in an inverse cascade[3]. Global structures that emerge from turbulent plasmas can be found in the laboratory[4] and in astrophysical settings; for example, the cosmic magnetic field[5,6], collisionless shocks in supernova remnants[7] and the internal structures of newly formed stars known as Herbig–Haro objects[8]. Here we show that large, stable electromagnetic field structures can also arise within counter-streaming supersonic plasmas in the laboratory. These surprising structures, formed by a yet unexplained mechanism, are predominantly oriented transverse to the primary flow direction, extend for much larger distances than the intrinsic plasma spatial scales and persist for much longer than the plasma kinetic timescales. Our results

Design of NIF experiment

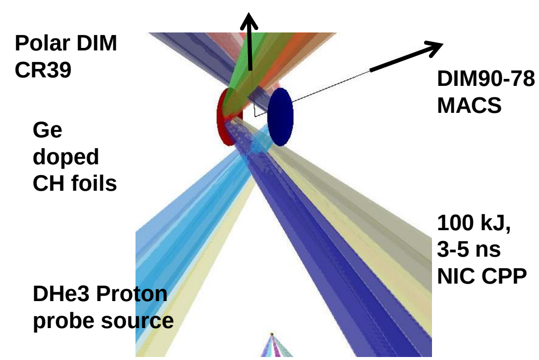

NIF will extend pair-plasma experiments to study of charge neutral systems (PI: H. Chen (LLNL))

Pair number vs. laser energy

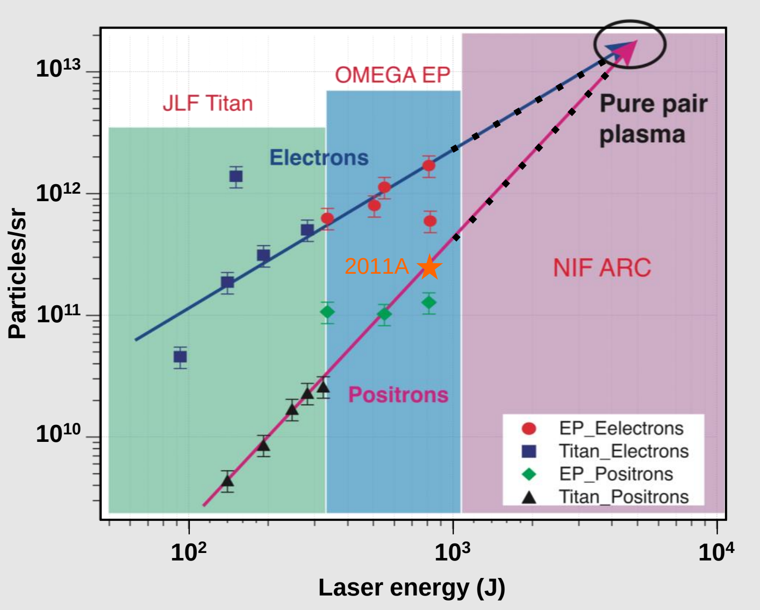

Positron jet vs. electron jet density

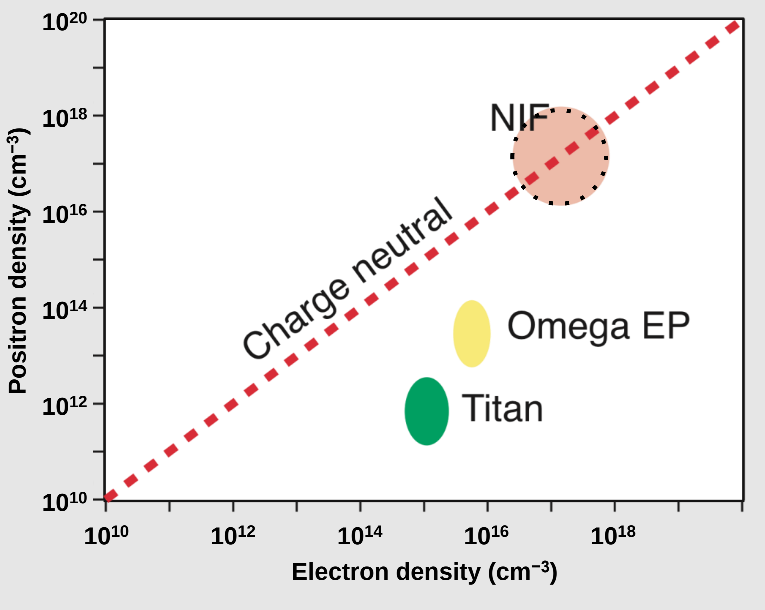

Bethe-Heitler process is dominant mechanism for production of e-/e+ pairs

NIF pair-plasma experiments will be the culmination of a multi-year, worldwide effort

Titan laser (LLNL)
1-10 ps, 100-350 J
5-10 shots/day

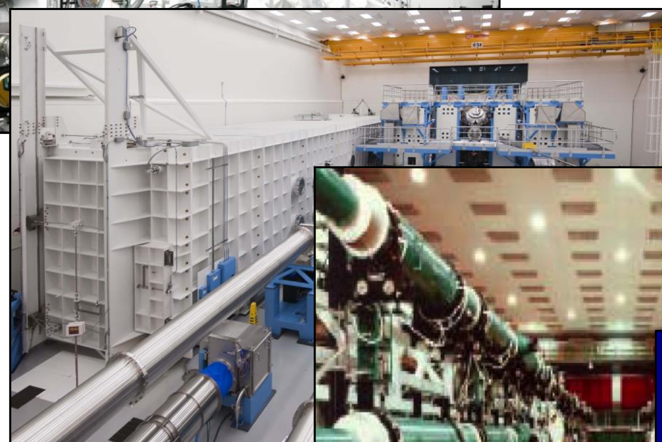

Omega EP (LLE)
1-10 ps, up to 1.3 kJ
5 shots/day

Gekko (ILE)
4 beams, 1 ps, ~1 kJ
Shots in 2012

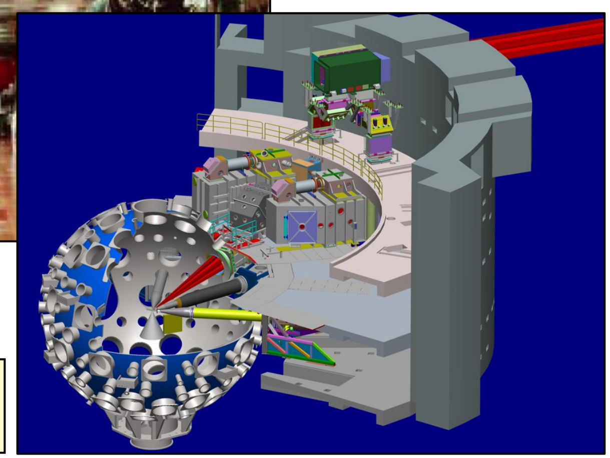

NIF ARC (LLNL)
1-50 ps, up to 10 kJ

- 9 experiments conducted in the past year at Titan, Omega, Gekko, Orion (UK)
- 3 published papers, 2 submitted
- 2 theses in progress

We successfully fielded first NIF Gbar EOS fundamental science experiment in early January 2013 (N130103)

Gbar EOS
Experimental configuration

X-ray Thomson Scattering

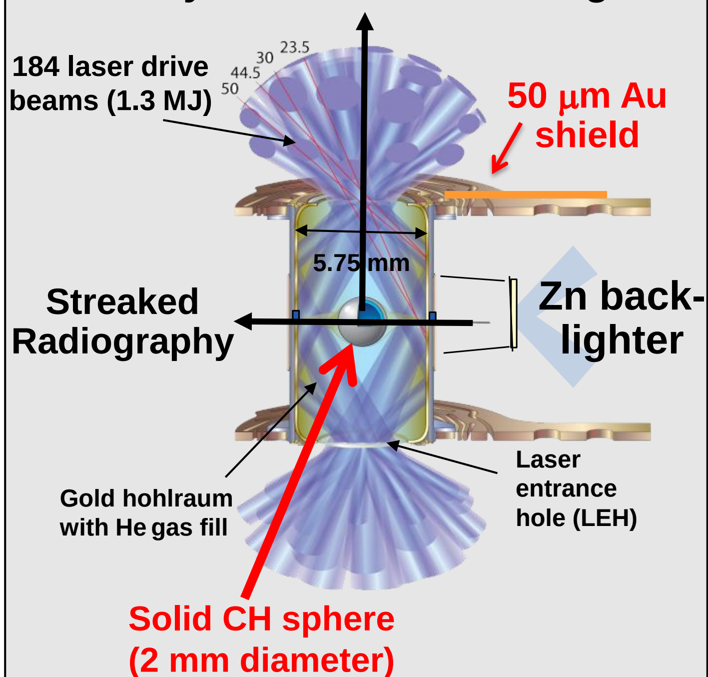

Streaked radiograph in 90-78

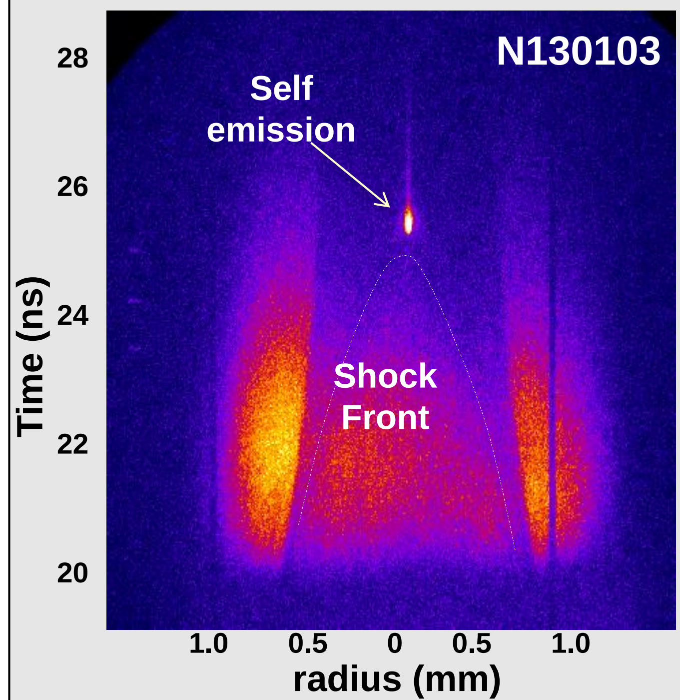

Shock speed reaches 220 km/s at r = 150 um

First NIF Gbar EOS experiment demonstrated Hugoniot measurement at ~10x higher pressures compared to NOVA data

Absolute shock Hugoniot measurements for CH

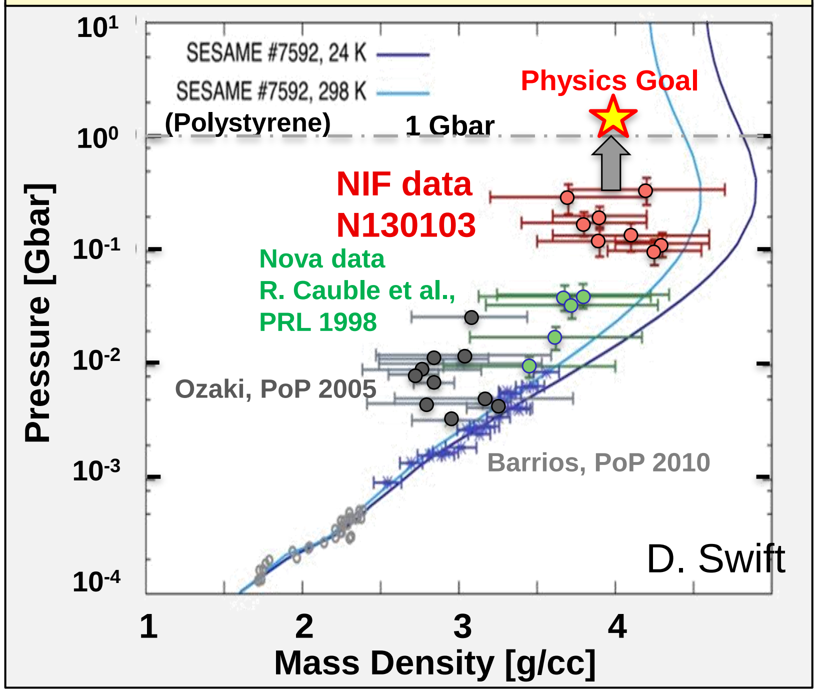

- **More detailed data analysis in progress**
- **N130103 was cryogenic expt., previous data at ambient temperature**
- **Need to increase hohlraum drive to reach Gbar pressure in ingoing shockwave**

Further experiments are planned this summer

Summary: Science on HED facilities is growing rapidly worldwide- please join us!

HiPER (EU)

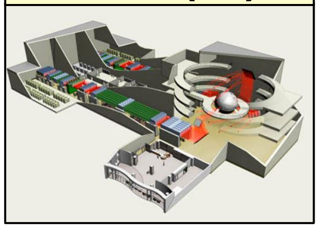

NIF Laser

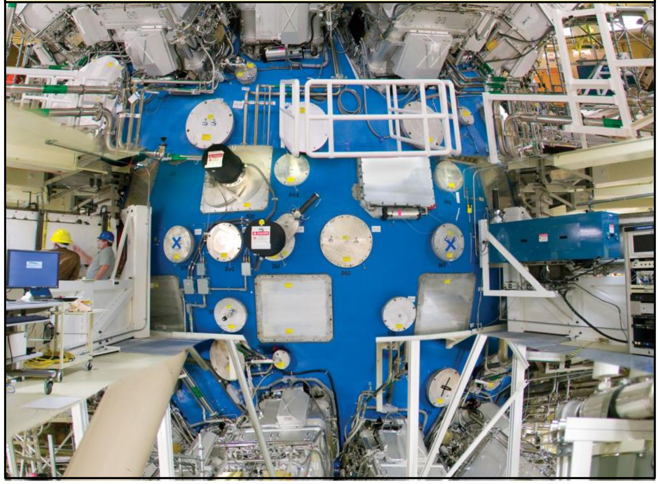

ORION (UK)

LMJ (France)

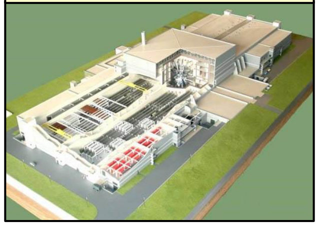

Vulcan (UK)

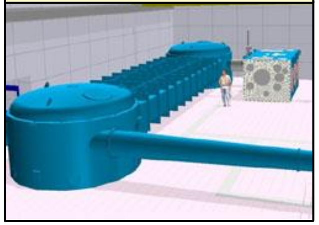

SG-III (China)

FIREX (Japan)

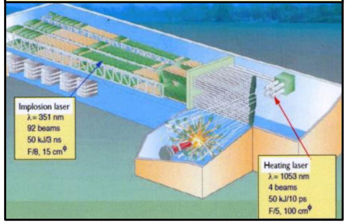

UFL-2M (Russia)

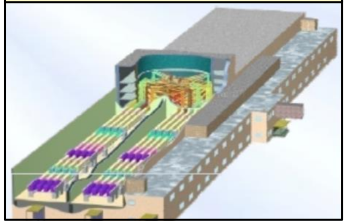

NIF will be a premier international center for experimental science

CERN

Chandra x-ray Observatory

APS

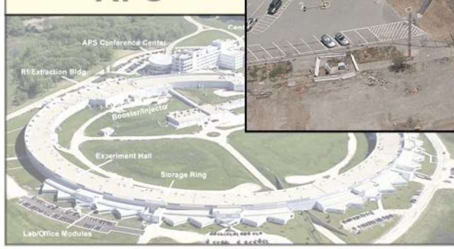

SLAC

The shock front can be clearly identified for radii > 150 um

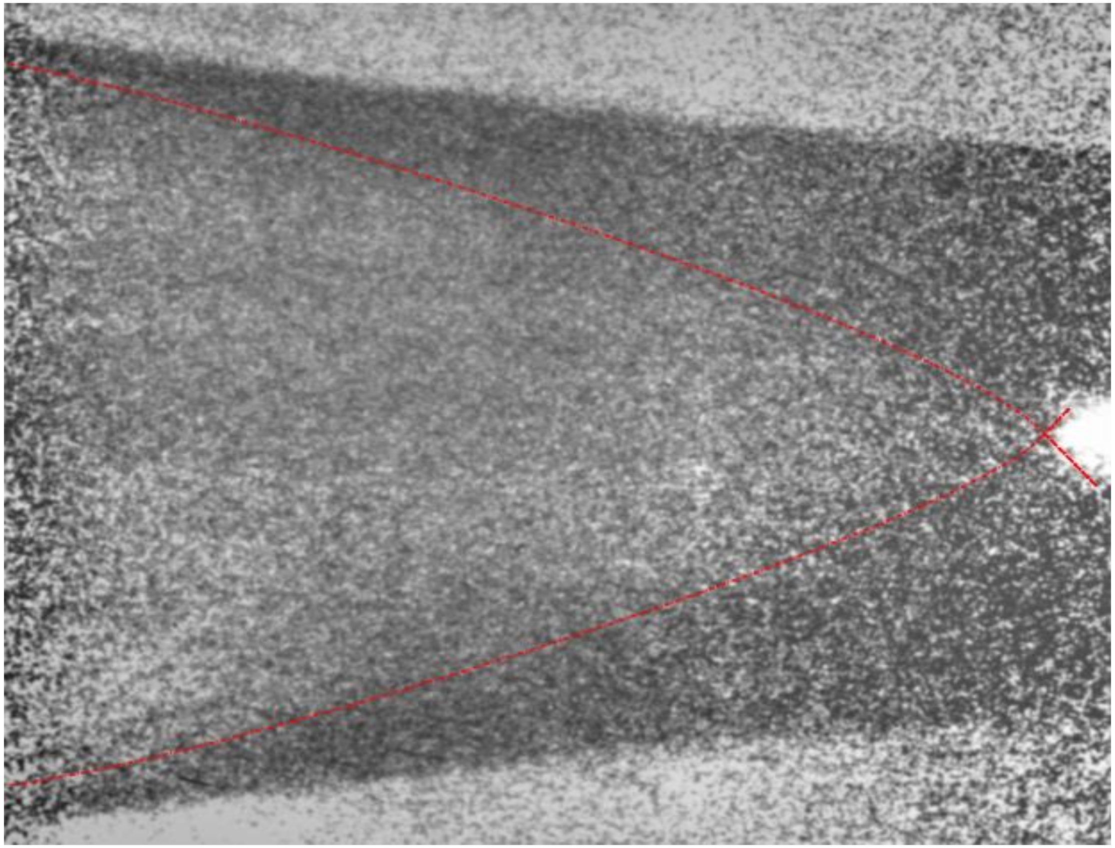

time

Shock speeds up to 220 km/s at r = 150 um, and up to 260 km/s at shock convergence

Hydrodynamics

The first university experiments at NIF were conducted to study effect of radiative shock on supernova hydrodynamics

Radiative effects on the Rayleigh-Taylor instability is relevant to core-collapse, red supergiant (Kuranz, Park et al)

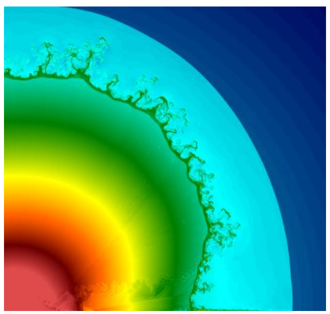

(SN simulation by Plewa)

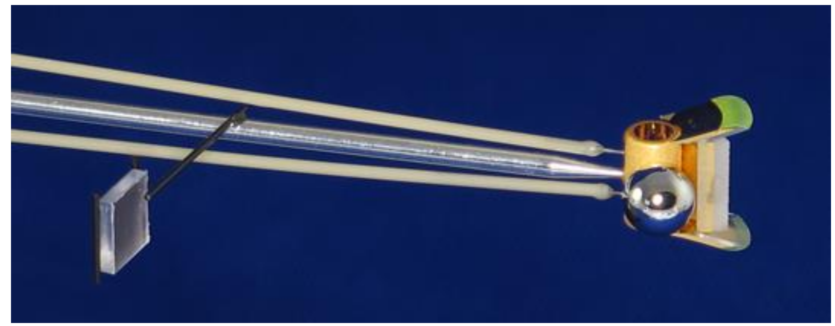

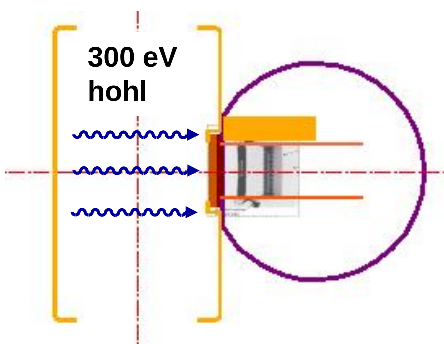

Backlighter development October 27, 2009

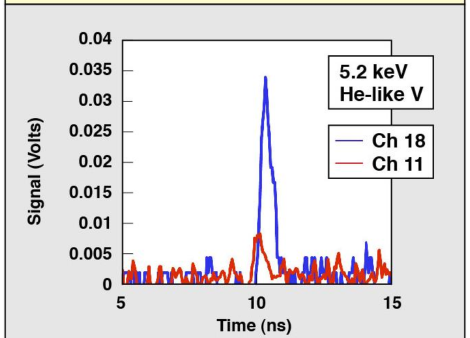

Conversion efficiency of ~0.4% measured in both channels—agrees with expectation

Drive development November 24, 2009

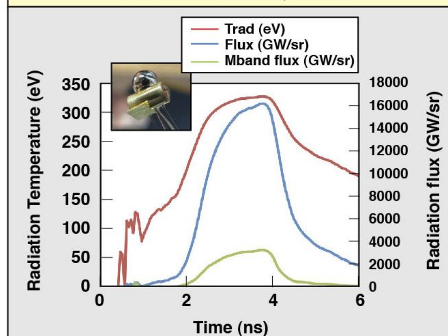

Highest drive ever measured in gas-filled hohlraum

Integrated experiment will be performed this FY

70

Materials

Jupiter/Omega results discovered a new solid-solid phase transition in MgO - effect on planetary structure

(Fig. 3A). Pt deposition resulted in three distinct levels of contrast that reflect the surface height, with the lowest level being the original Au terraces (Fig. 3B). The same three-level structure was observed independently of deposition time up to 500 s (Fig. 3C). The middle contrast level corresponds to a high density of Pt islands that covered ~85% of the Au surface, with a step height of ~0.24 nm, consistent with XPS results. Inspection with a higher rendering contrast revealed a ~10% coverage of a second layer of small Pt islands with a step height ranging between 0.23 and 0.26 nm (Fig. 3D). Step positions associated with the flame-annealed substrate were preserved, with negligible expansion or overgrowth of the 2D Pt islands occurring beyond the original step edge. The lateral span of the Pt islands was 2.02 ± 0.38 nm, corresponding to an area of 4.23 ± 1.97 nm^2. Incipient coalescence of the islands was constrained by surrounding (dark) narrow channels, 2.1 ± 0.25 nm wide, that account for the remaining Pt-free portion of the first layer. The reentrant channels correspond to open Au terrace sites that were surrounded by adjacent Pt islands in what amounted to a huge increase in step density relative to the original substrate, the net geometric or electronic effect of which was to block further Pt deposition. The chemical nature of the inter-island region was assayed by exploiting the distinctive voltammetry of Pt and Au with respect to H_{upd} and oxide formation and reduction (fig. S2 and supplementary text).

Similar three-level Pt overlayers have been observed for monolayer films produced by molecular beam epitaxy (MBE) deposition at 0.05 monolayers/min (*20*). Pt-Au intermixing driven by the decrease in surface energy that accompanies Au surface segregation was evident. In the present work, Pt monolayer formation was effectively complete within 1 s, giving a growth rate three orders of magnitude greater than in the MBE-STM study. Exchange of the deposited Pt with the underlying Au substrate was expected to be less developed. However, intermixing and possible chemical contrast (i.e., the ligand effect) were evident on limited sections of the surface that were correlated with the original faulted geometry of the partially reconstructed Au surface. Upon lifting of the reconstruction, the excess Au atoms expelled mark the original fault location as linear 1D surface defects in the Pt overlayer (Fig. 3E). A simplified schematic of the self-terminating Pt deposition process in Fig. 3F describes how the H_{upd} accompanying incremental expansion of the 2D Pt islands can hinder the development of a second Pt layer, presumably by perturbation of the overlying water structure (*17*). This rapid process resulted in a much higher Pt island coverage than has been obtained by other methods, such as galvanic exchange reactions.

Because the saturated H_{upd} coverage is the agent of termination, reactivation for further Pt deposition was possible by removing the upd layer by sweeping or stepping the potential to positive values, e.g., >+0.2 V_{SSCE}, where negligible Pt deposition occurs. Sequential pulsing between +0.4 V_{SSCE} and –0.8 V_{SSCE} enabled Pt monolayer deposition to be controlled in a digital manner. EQCM was used to track the mass gain, showing two net increments per cycle (Fig. 4A). We attributed the mass gain to a combination of Pt deposition [486 ng/cm^2 for a monolayer of Pt(111)], anion adsorption and desorption (41 ng/cm^2 for 7 × 10^{14} Cl^- ion/cm^2, 117 ng/cm^2 for a 0.14 fractional coverage of $PtCl_4^{2-}$) (*7*, *21*), and coupling to other double-layer components such as water. The anionic mass increments were expected to be asymmetric for the first cycle on the Au surface, but once it was covered, subsequent cycles only involved Pt surface chemistry. After correcting for the electroactive surface area of the Au electrode ($A_{real}/A_{geometric}$ = 1.2, derived from reductive desorption of Au oxide in perchloric acid), the net mass gain for each cycle indicates that a near-pseudomorphic layer of Pt was deposited. XPS analysis of Pt films grown in various deposition cycles gave remarkably good agreement with EQCM data (Fig. 4B). The ability to rapidly manipulate potential and double-layer structure, as opposed to the exchange of reactants, offers simplicity, substantially improved process efficiency, and far greater process speed than other surface-limited deposition methods.

References and Notes

1. F. T. Wagner, R. Lakshmanan, M. F. Mathias, *J. Phys. Chem. Lett.* **1**, 2204 (2010).
2. M. K. Debe, *Nature* **486**, 43 (2012).
3. M. T. M. Koper, Ed., *Fuel Cell Catalysis, A Surface Science Approach* (Wiley, Hoboken, NJ, 2009).
4. V. R. Stamenkovic *et al.*, *Nat. Mater.* **6**, 241 (2007).
5. R. R. Adzic *et al.*, *Top. Catal.* **46**, 249 (2007).
6. T. Michely, J. Krug, *Islands, Mounds and Atoms, Patterns and Processes in Crystal Growth Far from Equilibrium* (Springer Series in Surface Science, V42, Springer, New York, 2003).
7. H. F. Waibel, M. Kleinert, L. A. Kibler, D. M. Kolb, *Electrochim. Acta* **47**, 1461 (2002).
8. T. Kondo *et al.*, *Electrochim. Acta* **55**, 8302 (2010).
9. I. Bakos, S. Szabo, T. Pajkossy, *J. Solid State Electrochem.* **15**, 2453 (2011).
10. S. R. Brankovic, J. X. Wang, R. R. Adzic, *Surf. Sci.* **474**, L173 (2001).
11. D. Gokcen, S.-E. Bae, S. R. Brankovic, *Electrochim. Acta* **56**, 5545 (2011).
12. B. W. Gregory, J. L. Stickney, *J. Electroanal. Chem.* **300**, 543 (1991).
13. A. J. Gregory, W. Levason, R. E. Noftle, R. Le Penven, D. Pletcher, *J. Electroanal. Chem.* **399**, 105 (1995).
14. See supplementary materials on *Science* Online.
15. N. Garcia-Araez, V. Climent, E. Herrero, J. Feliu, J. Lipkowski, *J. Electroanal. Chem.* **582**, 76 (2005).
16. D. Strmcnik, D. Tripkovic, D. van der Vliet, V. Stamenkovic, N. M. Markovic, *Electrochem. Commun.* **10**, 1602 (2008).
17. T. Roman, A. Groß, Structure of water layers on hydrogen-covered Pt electrodes. *Cataly. Today*; http://dx.doi.org/10.1016/j.cattod.2012.06.001 (2012).
18. G. Jerkiewicz, G. Vatankhah, S. Tanaka, J. Lessard, *Langmuir* **27**, 4220 (2011).
19. P. J. Cumpson, M. P. Seah, *Surf. Interface Anal.* **25**, 430 (1997).
20. M. O. Pedersen *et al.*, *Surf. Sci.* **426**, 395 (1999).
21. Y. Nagahara *et al.*, *J. Phys. Chem. B* **108**, 3224 (2004).

Acknowledgments: We thank J. J. Mallett for his early observations on the difficulty of electrodepositing Pt films at negative potentials. This work was supported by NIST–Material Measurement Laboratory programs. The x-ray photoelectron spectrometer was provided by NIST–American Recovery and Reinvestment Act funds. Y.L. thanks the NIST–National Research Council Postdoctoral Fellowship Program for support. NIST has filed a provisional patent application (Atomic Layer Deposition of Pt from Aqueous Solutions) based on this work.

Supplementary Materials
www.sciencemag.org/cgi/content/full/338/6112/1327/DC1
Materials and Methods
Supplementary Text
Figs. S1 and S2
References (*22*–*26*)

16 August 2012; accepted 17 October 2012
10.1126/science.1228925

Phase Transformations and Metallization of Magnesium Oxide at High Pressure and Temperature

R. Stewart McWilliams,[1,2]*† Dylan K. Spaulding,[3]‡ Jon H. Eggert,[4] Peter M. Celliers,[4] Damien G. Hicks,[4] Raymond F. Smith,[4] Gilbert W. Collins,[4] Raymond Jeanloz[3,5]

Magnesium oxide (MgO) is representative of the rocky materials comprising the mantles of terrestrial planets, such that its properties at high temperatures and pressures reflect the nature of planetary interiors. Shock-compression experiments on MgO to pressures of 1.4 terapascals (TPa) reveal a sequence of two phase transformations: from B1 (sodium chloride) to B2 (cesium chloride) crystal structures above 0.36 TPa, and from electrically insulating solid to metallic liquid above 0.60 TPa. The transitions exhibit large latent heats that are likely to affect the structure and evolution of super-Earths. Together with data on other oxide liquids, we conclude that magmas deep inside terrestrial planets can be electrically conductive, enabling magnetic field–producing dynamo action within oxide-rich regions and blurring the distinction between planetary mantles and cores.

Magnesium oxide (MgO) is among the simplest oxides constituting the rocky mantles of terrestrial planets such as Earth and the cores of Jupiter and other giant planets. Present in Earth's mantle as an end-member component of the mineral (Mg,Fe)O magnesiowüstite,

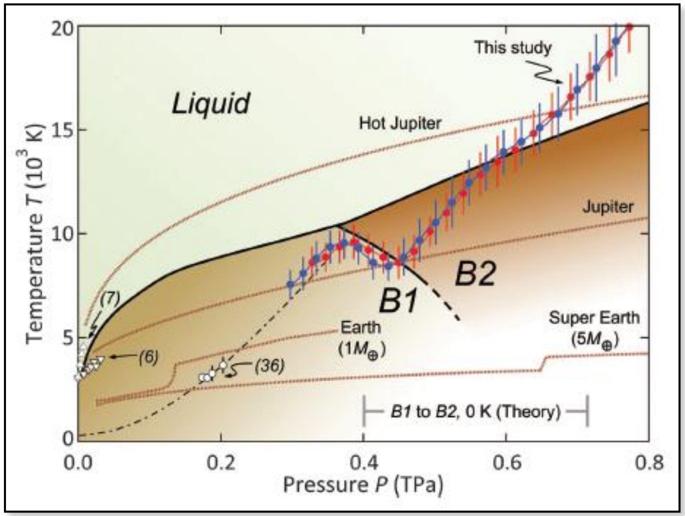

- Established solid-solid phase transition for the first time
- Metallization above 6 Mbar – dynamo effect possible in deep mantles
- Unexpectedly large latent heats

Stewart, et al.
Coppari, et al.

High intensity interactions

JLF results on hot electron production

PRL 108, 115004 (2012) PHYSICAL REVIEW LETTERS week ending 16 MARCH 2012

Hot Electron Temperature and Coupling Efficiency Scaling with Prepulse for Cone-Guided Fast Ignition

T. Ma,[1,2] H. Sawada,[2] P. K. Patel,[1] C. D. Chen,[1] L. Divol,[1] D. P. Higginson,[1,2] A. J. Kemp,[1] M. H. Key,[1] D. J. Larson,[1] S. Le Pape,[1] A. Link,[1,3] A. G. MacPhee,[1] H. S. McLean,[1] Y. Ping,[1] R. B. Stephens,[4] S. C. Wilks,[1] and F. N. Beg[2]
[1]*Lawrence Livermore National Laboratory, Livermore, California 94550, USA*
[2]*University of California-San Diego, La Jolla, California 92093, USA*
[3]*The Ohio State University, Columbus, Ohio 43210, USA*
[4]*General Atomics, San Diego, California 92186, USA*
(Received 3 December 2011; published 16 March 2012)

The effect of increasing prepulse energy levels on the energy spectrum and coupling into forward-going electrons is evaluated in a cone-guided fast-ignition relevant geometry using cone-wire targets irradiated with a high intensity (10^{20} W/cm^2) laser pulse. Hot electron temperature and flux are inferred from $K\alpha$ images and yields using hybrid particle-in-cell simulations. A two-temperature distribution of hot electrons was required to fit the full profile, with the ratio of energy in a higher energy (MeV) component increasing with a larger prepulse. As prepulse energies were increased from 8 mJ to 1 J, overall coupling from laser to all hot electrons entering the wire was found to fall from 8.4% to 2.5% while coupling into only the 1–3 MeV electrons dropped from 0.57% to 0.03%.

DOI: 10.1103/PhysRevLett.108.115004 PACS numbers: 52.50.Jm, 52.38.Kd, 52.38.Mf, 52.70.La

Fast Ignition (FI) [1,2] is an approach to inertial confinement fusion (ICF), in which a precompressed deuterium-tritium fuel is rapidly driven to ignition by an external heat source. This scheme can ignite lower density fuel leading, in principle, to higher gains than possible with conventional ignition. In the reentrant cone approach to FI, a hollow cone is embedded in the fuel capsule to provide an open evacuated path free of coronal plasma for an intense laser beam to generate a flux of energetic electrons at the tip of the cone which can then propagate to the compressed fuel core. However, the presence of preformed plasma in the cone, arising from the inherent laser prepulse which ablates the inner cone wall, can strongly affect the spatial, energy-spectral, and angular characteristics of these laser-generated hot electrons and thus the efficiency with which their energy can be coupled to the core.

Previous works by Baton *et al.* [3] and Van Woerkom *et al.* [4] showed that significant prepulse could have a detrimental effect on coupling beyond the cone tip. MacPhee *et al.* [5] demonstrated that even a small prepulse could result in significant filamentation of the laser beam in the preplasma, limiting the penetration of the laser, and accelerating energetic electrons transversely. These results were achieved using either imaging of $K\alpha$ x-ray emission from the cone target itself or measuring the intensity of the $K\alpha$ spot in a region beyond the cone tip. However, while these techniques provided a spatial distribution of $K\alpha$ in various areas of the interaction, no spectral information regarding the electron flux could be inferred. Comparisons of preplasma versus no preplasma conditions by Baton *et al.* were achieved by doubling the fundamental laser frequency to create a high contrast. This provided a clean interaction surface for the main laser, but complicated the comparison, as the absorption mechanisms would be different for the very different $I\lambda^2$. In the MacPhee *et al.* study, electrons were electrostatically confined within the isolated cone target. The significant amount of recirculation of the hot electrons within the cone walls and plasma allows only limited conclusion of the electron source at the cone tip in either the experiment or simulations.

In this Letter, we present the first quantitative scaling of coupling as a function of prepulse in an intense laser-cone interaction. Through the use of cone-wire targets [6], we demonstrate the existence of a two-temperature hot electron distribution within the target and characterize its flux and energy spectrum entering a 40 μm diameter wire at the cone tip, and correlate these quantities with the amount of preformed plasma in the cone.

The experiment was performed on the Titan laser at LLNL, of $\lambda_0 = 1.054$ μm wavelength, 150 ± 10 J, focused to an 8 μm full width at half maximum (FWHM) focal spot in a 0.7 ± 0.2 ps pulse length. The intrinsic prepulse of the laser was measured at 8 ± 3 mJ in a 1.7 ns duration pulse prior to the main beam. Varying prepulse levels, up to 1 J, were produced by injecting an auxiliary nanosecond-duration laser colinear with the main short pulse laser. This auxiliary laser had a similar focal spot distribution as the main beam and was timed to overlap the intrinsic prepulse.

The target, shown in Fig. 1, was a 1 mm long Au hollow cone with 30° full opening angle, 20 μm wall thickness, 30 μm internal tip diameter, and 11 μm tip thickness. A 1.5 mm long, 40 μm diameter Cu wire was glued to the outer cone tip. The wire diameter is chosen to match the nominal 40 μm optimum ignition hot spot diameter in a FI target [7], and its quasi 1D geometry allows for single shot

0031-9007/12/108(11)/115004(5) 115004-1

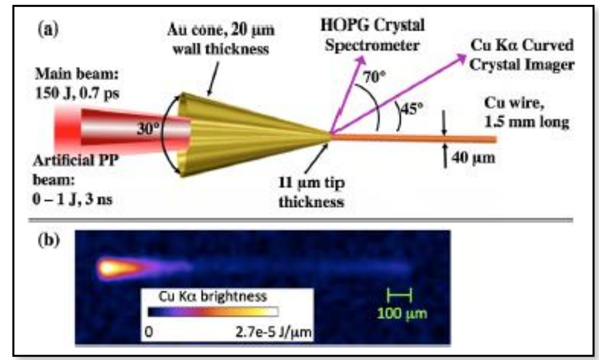

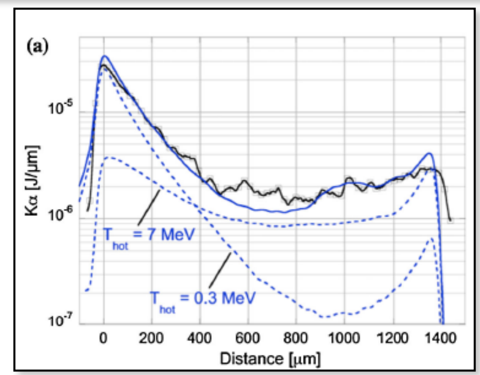

- Kα emission follows hot electrons in wire
- Find 2-temperature distribution required
- Laser-to-hot-electron efficiency measured

The categorization in the 2009 Office of Science "Basic Research Needs" report provides an effective means to categorize HEDS research

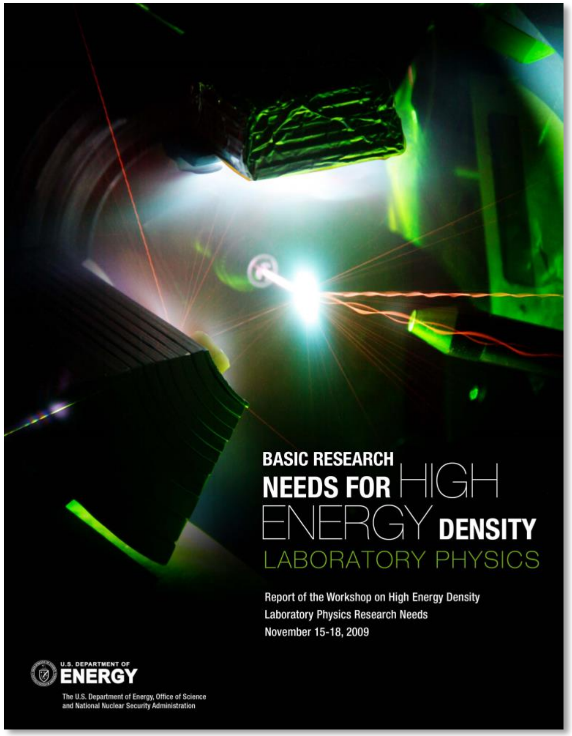

Major areas of technical interest:

- **High Energy Density Hydrodynamics**
- **Magnetized High Energy Density Plasma**
- **Nonlinear Optics of Plasmas**
- **Radiation-Dominated Dynamics and Material Properties**
- **Relativistic HED Plasmas and Intense Beam Physics**
- **Warm Dense Matter**
- **High-Z Multiply Ionized HED Atomic Physics**
- **Diagnostics**

Dramatic improvements in optical damage thresholds have been developed to enable high-energy opertions

Improvement in fused silica surface finish from 1997 to present

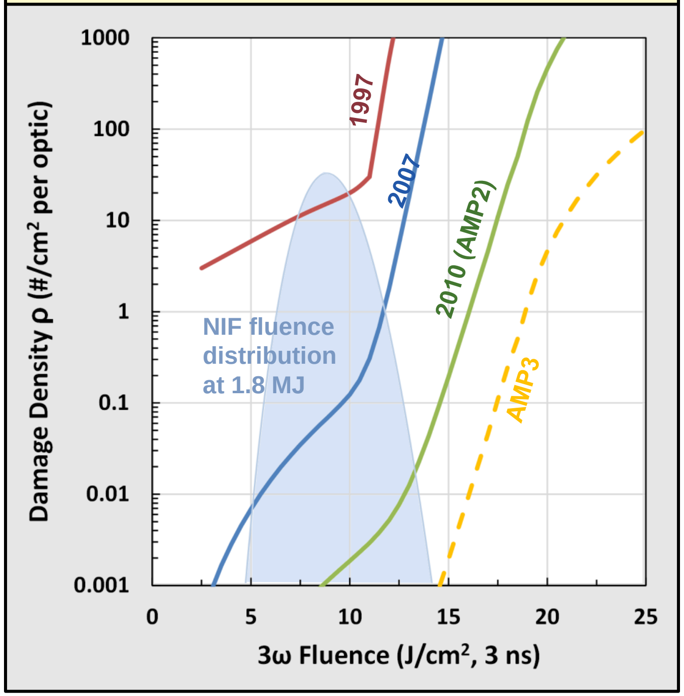

Improvement in damage initiation at 1.8 MJ, 3 ns

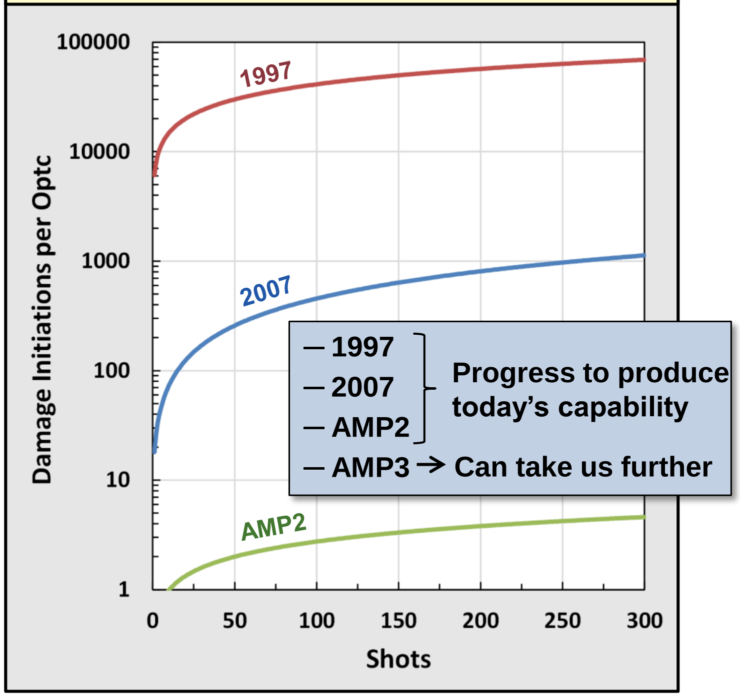

2003 NRC Report on High Energy Density Physics defines HED science as P> 1 Mbar (10^{11} J/m^3)

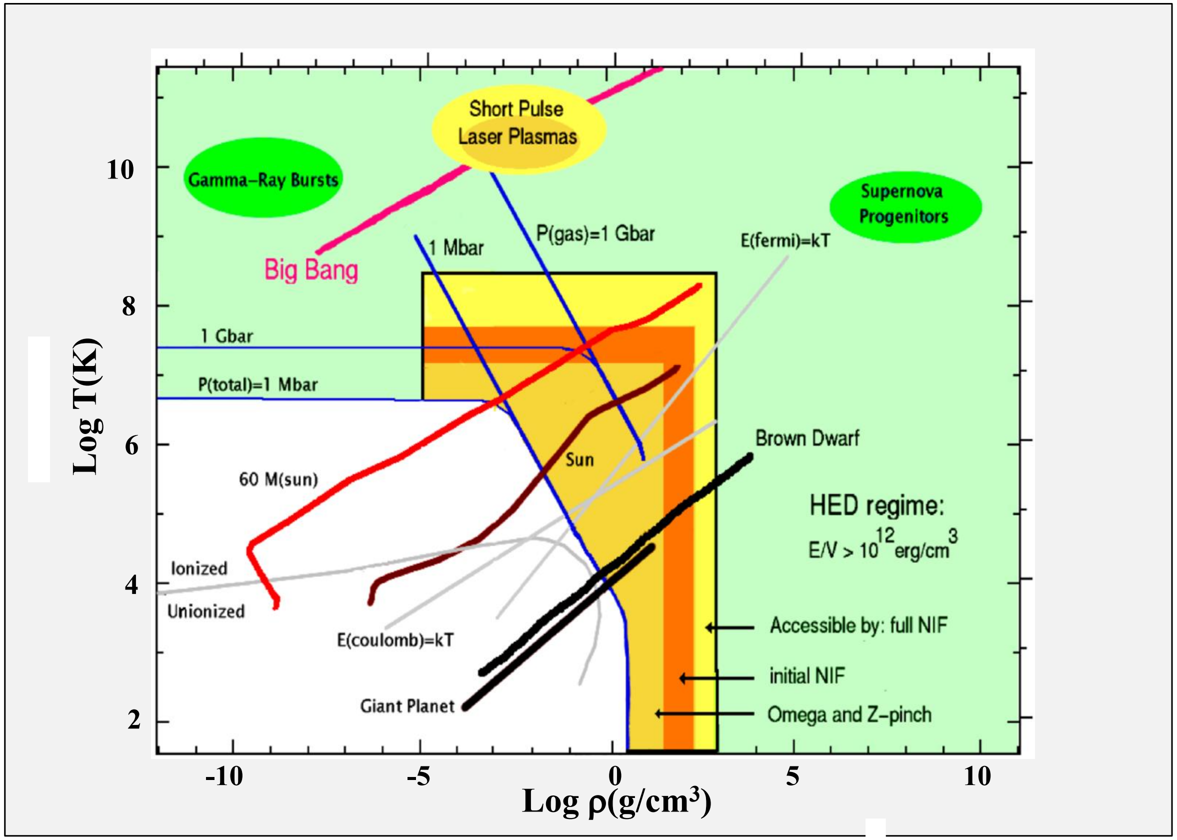

Recent data show that P4 asymmetry can be modified by extending the hohlraum length

Nominal length hohlraum

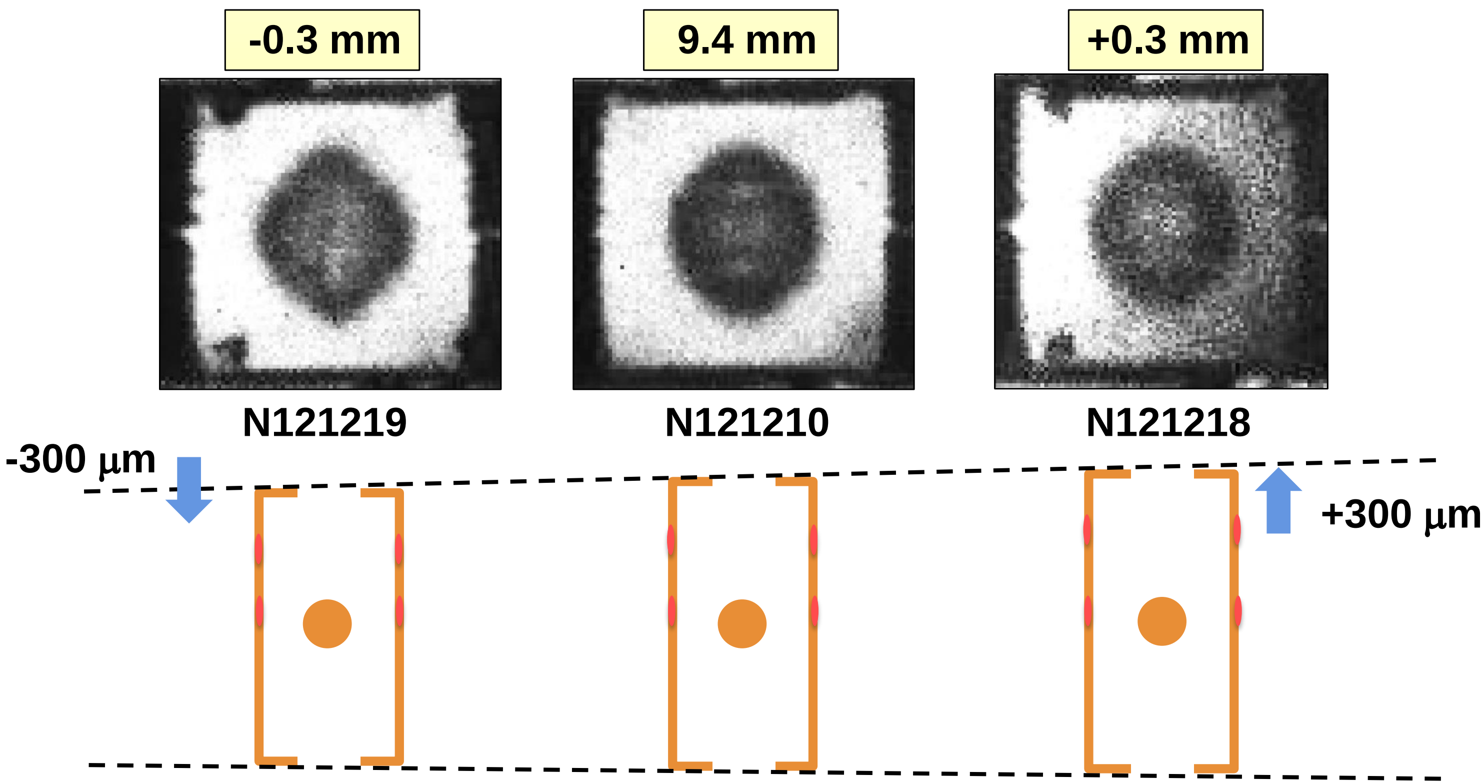

X-ray drive symmetry must be controlled to the ~1% level

NIF has conducted nearly 1300 shots since start of operations in spring 2009

Type	Purpose	Total
Target shots-	Stockpile Stewardship- Inertial confinement fusion	259
Program data	Stockpile Stewardship- HED science	145
	DOD and other national security	17
	Fundamental science	15
Target shots- Capabilities	Target diagnostics commissioning/calibration; Capability development; System qualification	191
Laser shots	Laser/optics performance and calibration	661
Total (through 6/4/13)		1288

NIF fundamental science experiments

Topic	PI Last	PI Institution
Carbon and Iron Equation of State	T. Duffy/ R. Jeanloz	Princeton/UCB
Supernova hydrodynamics- Radiative Effects (Rad SNRT)	C. Kuranz	Univ. of Michigan
Novel phases of compressed diamond	J. Wark/ J. Eggert	Oxford/LLNL
Nucleosynthesis and the s-process	L. Bernstein	LLNL
Rayleigh-Taylor instability and astrophysical implications (merged proposal)	A. Casner/ V. Smalyuk	CEA
	J. Kane	LLNL
Matter at ultra-high densities (merged proposal)	P. Neumayer	GSI
	R.Falcone	UC Berkeley
Hydrogen and methane at ultra-high pressures (merged proposal)	R. Jeanloz	UC Berkeley
	R. Hemley	Carnegie Institution of Washington
Diverging Supernova hydrodynamics	T. Plewa	FSU
Astrophysical collisionless shocks (merged proposal)	Y. Sakawa	Osaka University
	G. Gregori	Univ. of Oxford
Relativistic pair plasmas	H. Chen	LLNL